



Materials Science at Large Scale Facilities

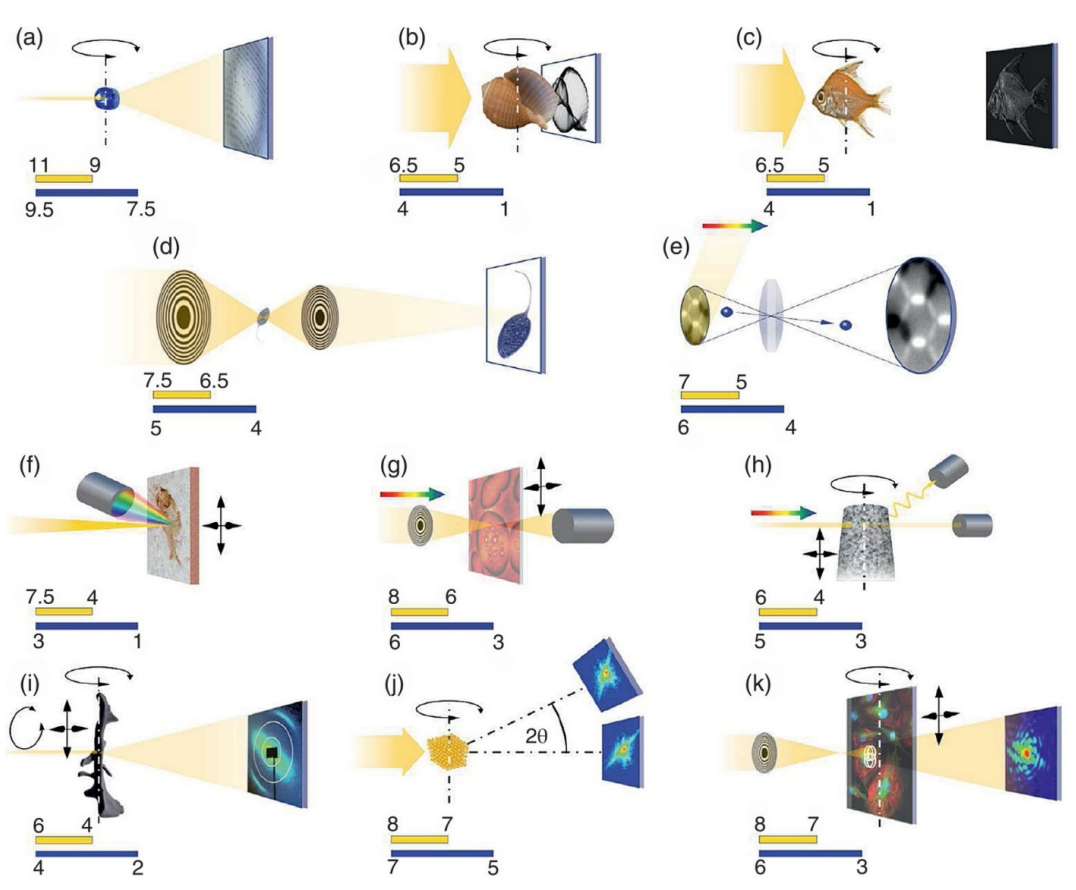
X-ray imaging

Imaging

- After his discovery of X-rays in 1885, Röntgen immediately discovered that these X-rays were also able to stain photographic plates.
- He demonstrated that objects of different thicknesses and density placed in the path of these rays showed differing degrees of transparency.
- First ever X-ray image from the hand of Swiss anatomist Albert von Kölliker
- Very first Nobel prize in Physics (in 1901)

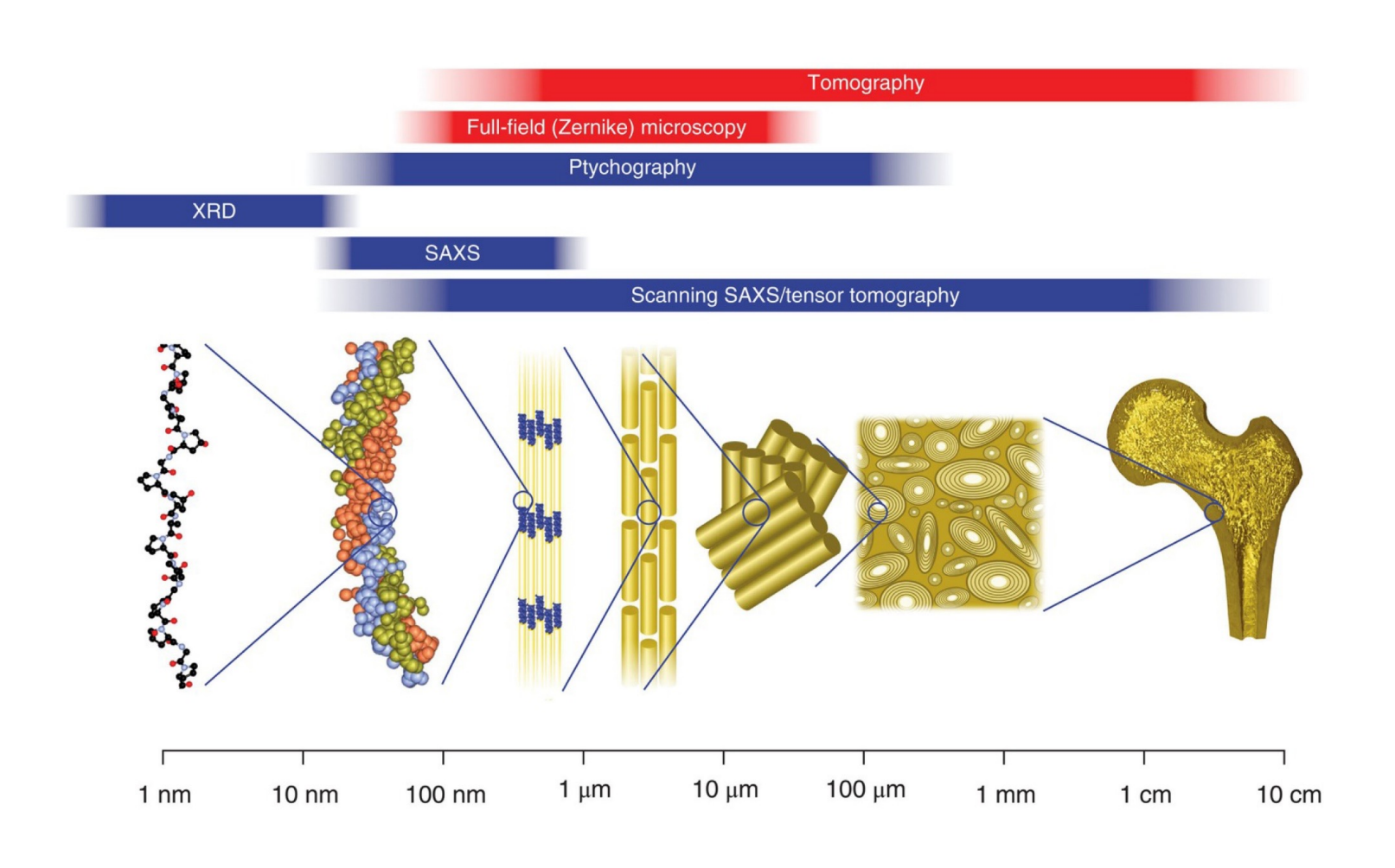


Many different types of imaging

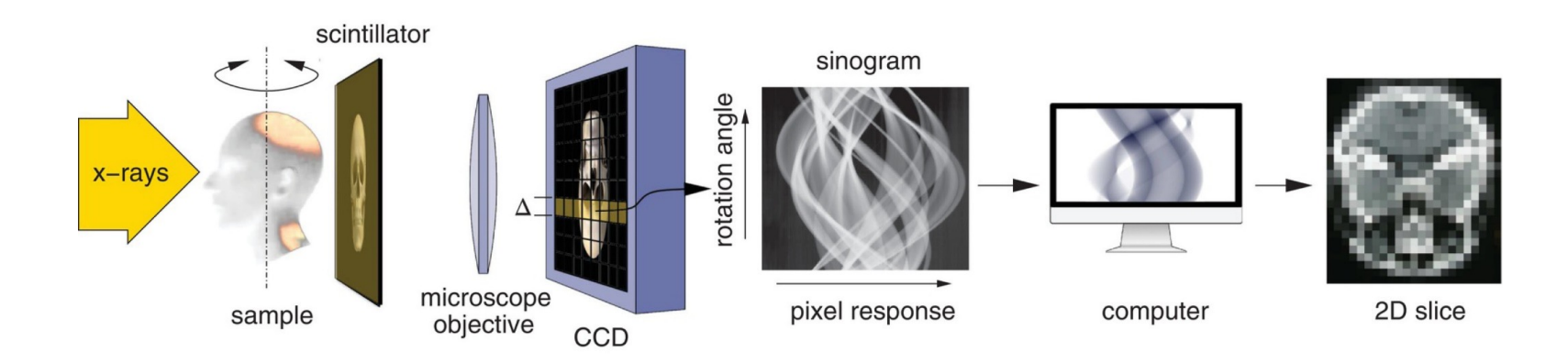


(a) X-ray diffraction; (b) absorption-contrast XTM; (c) phase-contrast XTM; (d) full-field hard-x-ray (including Zernike) microscopy; (e) PEEM/XMCD spectromicroscopy; (f) scanning XRF microspectroscopy; (g) STXM; (h) chemical line tomography; (i) scanning SAXS; (j) CXDI and Bragg CXDI; (k) ptychography/ptychographic tomography

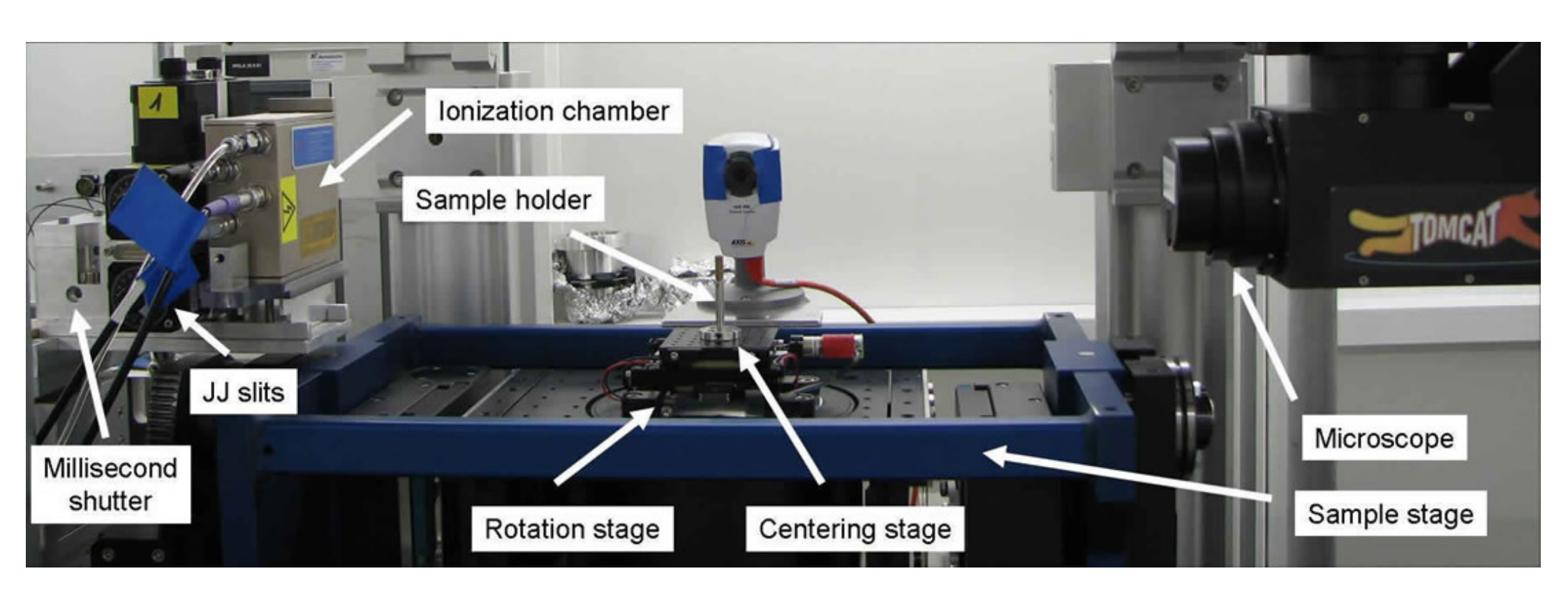
Let's go 3D



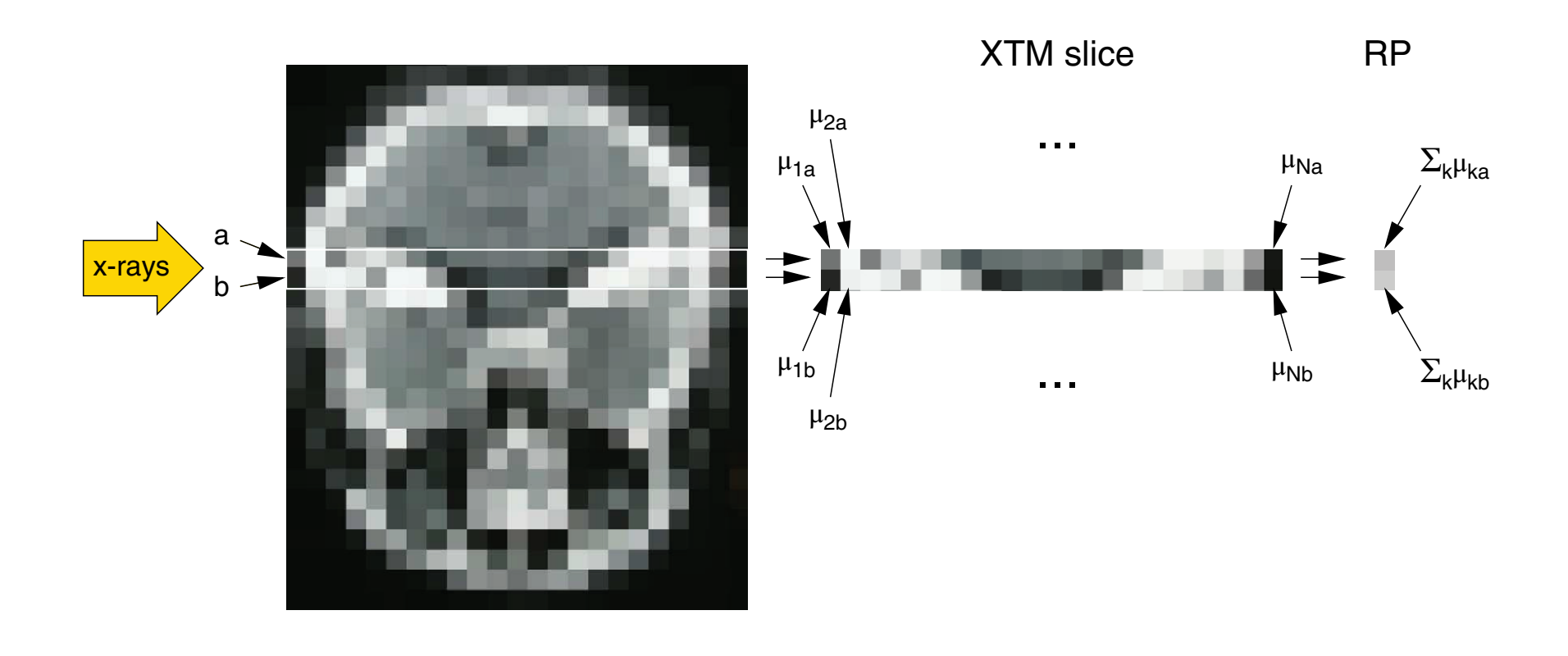
- The word 'tomography' is derived from the Greek words 'tomos' meaning 'to slice' and 'graph' meaning 'image'.
- The generation of a three-dimensional image by analysing several transmission radiographic projections taken of a specimen at different angles.
- Standard CT scans with resolution of the order of 0.5mm is very common. For instance, approximately 100 million CT scans per year are performed in the USA alone.



TOMCAT station at the SLS

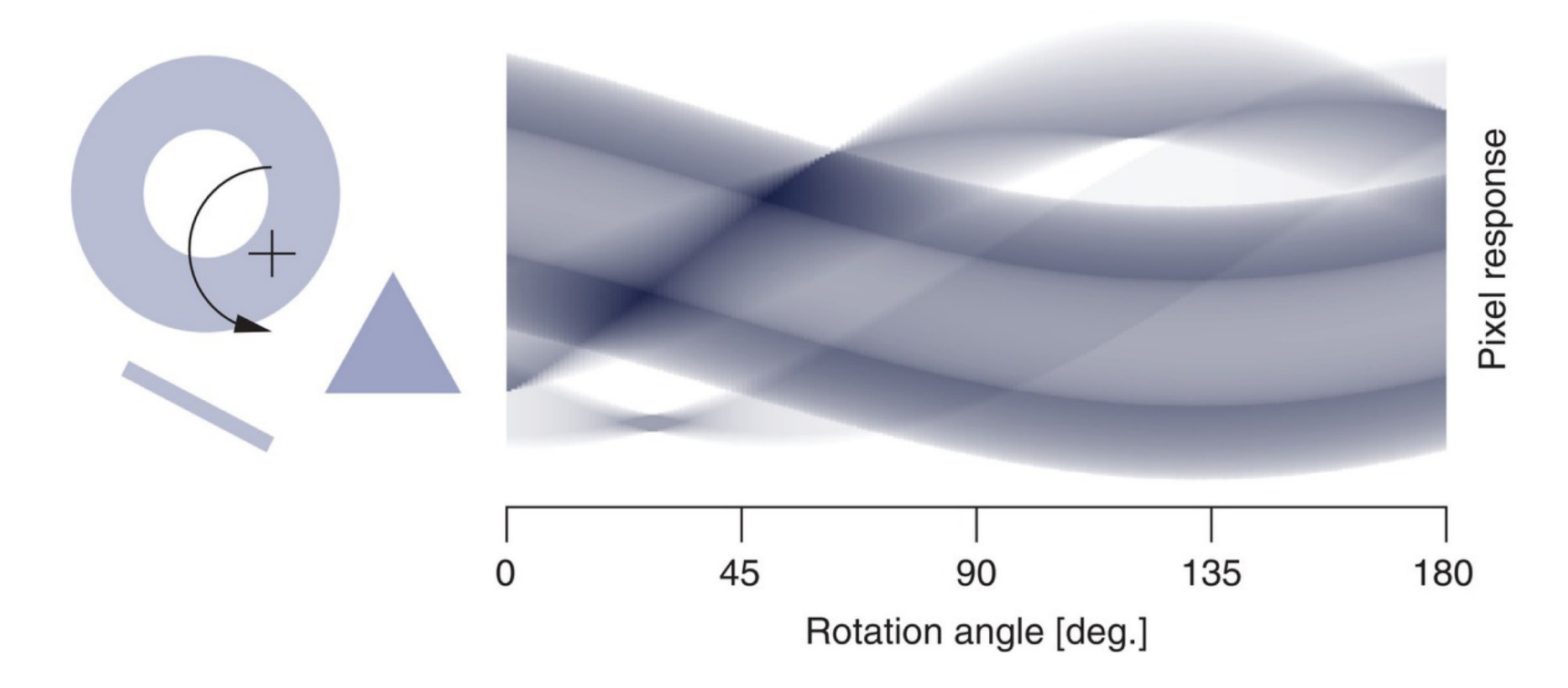


Tomographic vs radiographic imaging

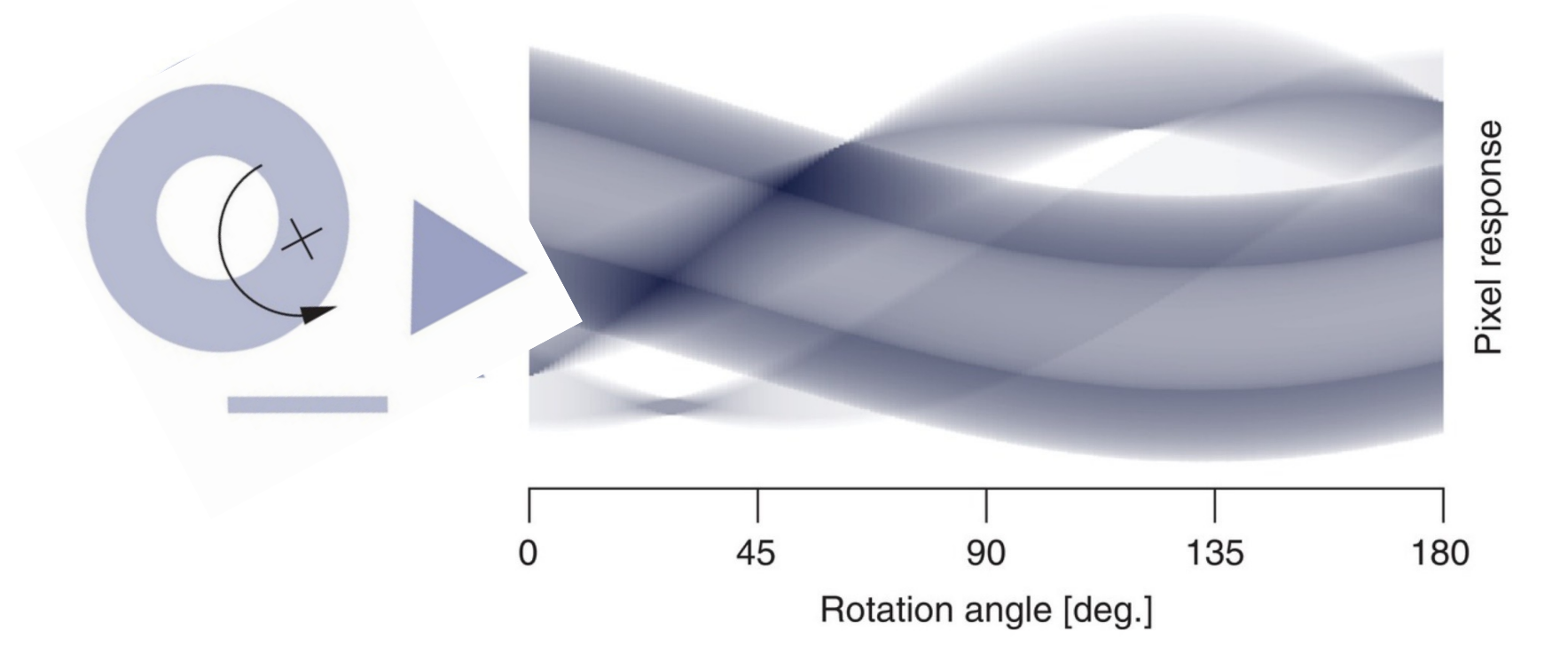


- The spatial resolution of the image is determined by:
 - the point-spread function of the scintillator
 - the magnification factor of the microscope objective optics M
 - the signal-to-noise ratio of the CCD image
 - the linear pixel size Δ and point-spread function of the CCD camera
- The number of projections N of the sample which must be recorded within the angular range is given by the so-called 'sampling theorem: $N = N_p \times \pi/2$, whereby N_p is the number of resolution elements in the row that provide transmission data.
- From each row in the CCD array, a tomogram is generated. To obtain this, the response of the *Np* pixels in the row as a function of rotation angle, known as a *sinogram*, is fed into a computer.

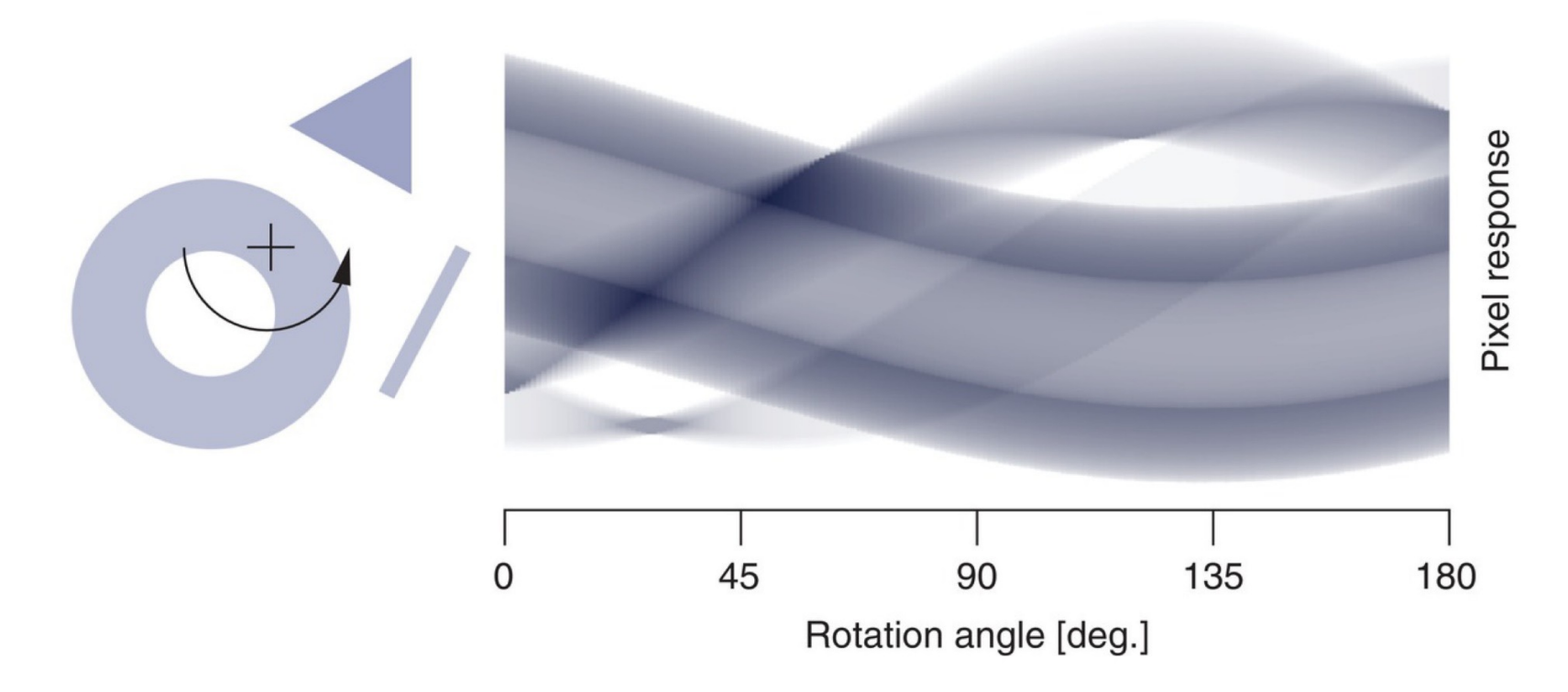
• The response of a line of pixels in the plane of three partially absorbing, simple geometrical two-dimensional objects as a function of their rotation around the crosshair between 0° and 180° results in the corresponding sinogram.

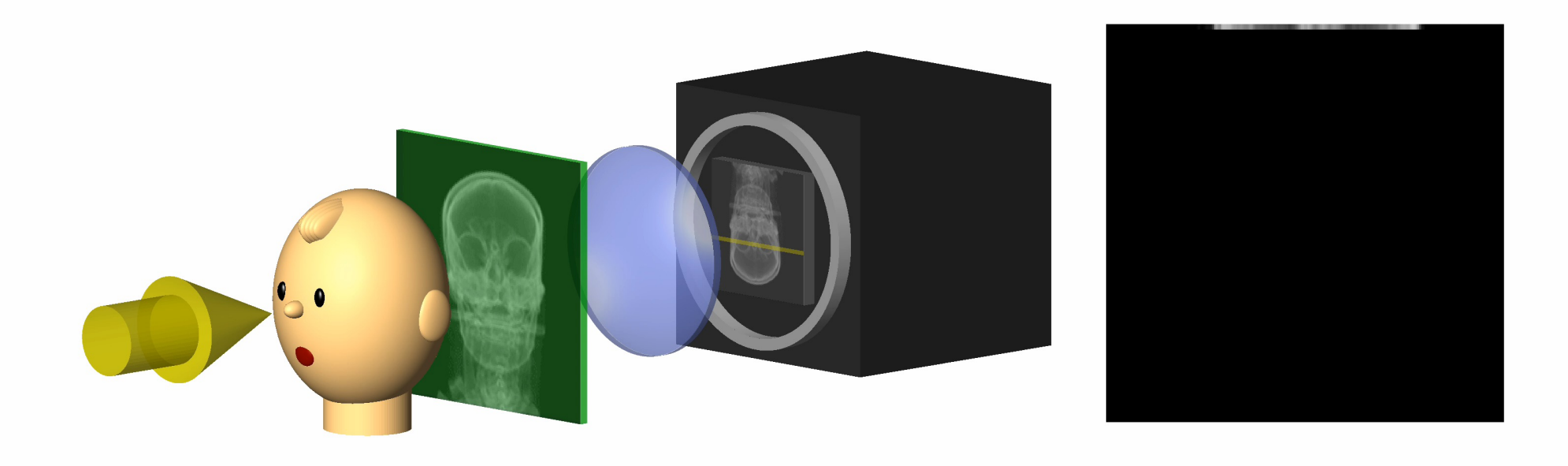


• The response of a line of pixels in the plane of three partially absorbing, simple geometrical two-dimensional objects as a function of their rotation around the crosshair between 0° and 180° results in the corresponding sinogram.



• The response of a line of pixels in the plane of three partially absorbing, simple geometrical two-dimensional objects as a function of their rotation around the crosshair between 0° and 180° results in the corresponding sinogram.





• The response of a detector pixel is proportional to the intensity of the transmitted x-rays that impinges upon it after travelling along a path $L = M\Delta z$ through an object.

$$I = I_0 e^{-\mu_1 \Delta z} e^{-\mu_2 \Delta z} e^{-\mu_3 \Delta z} \cdots e^{-\mu_M \Delta z}$$

$$=I_0\exp\left(-\sum_{k=1}^M\mu_k\Delta z\right).$$

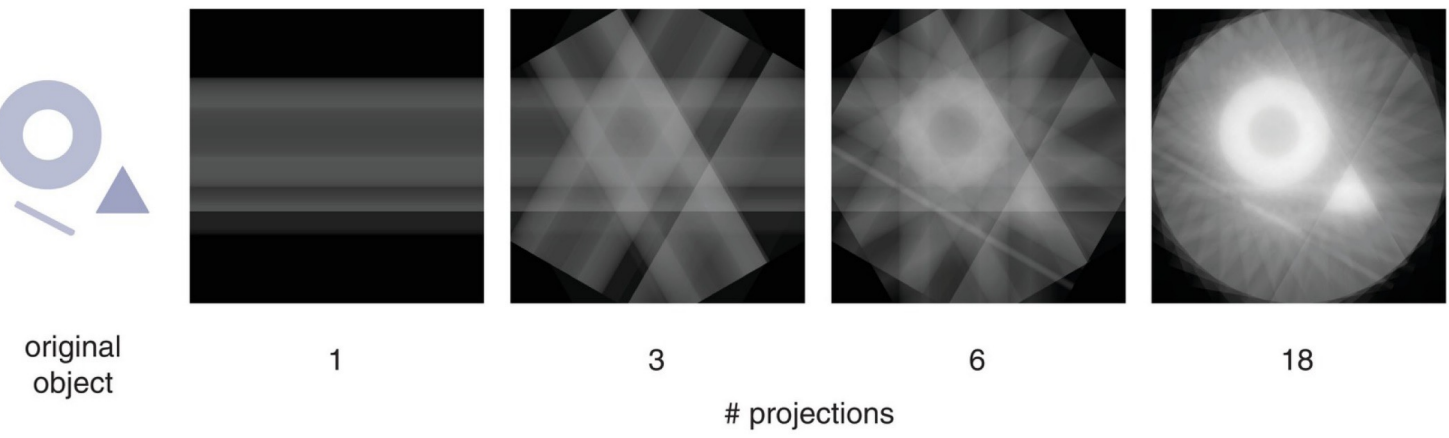
We define the projection measurement as:

$$p = -\ln\left(\frac{I}{I_0}\right) = \sum_{k=1}^{M} \mu_k \Delta z \approx \int_L \mu(z) dz$$

• *p* for a given pixel at a given angle is the line integral of the object's attenuation coefficient along the line *L*. Given these sets of line integrals for different angles, the task is to reconstruct the attenuation distribution throughout the entire object.

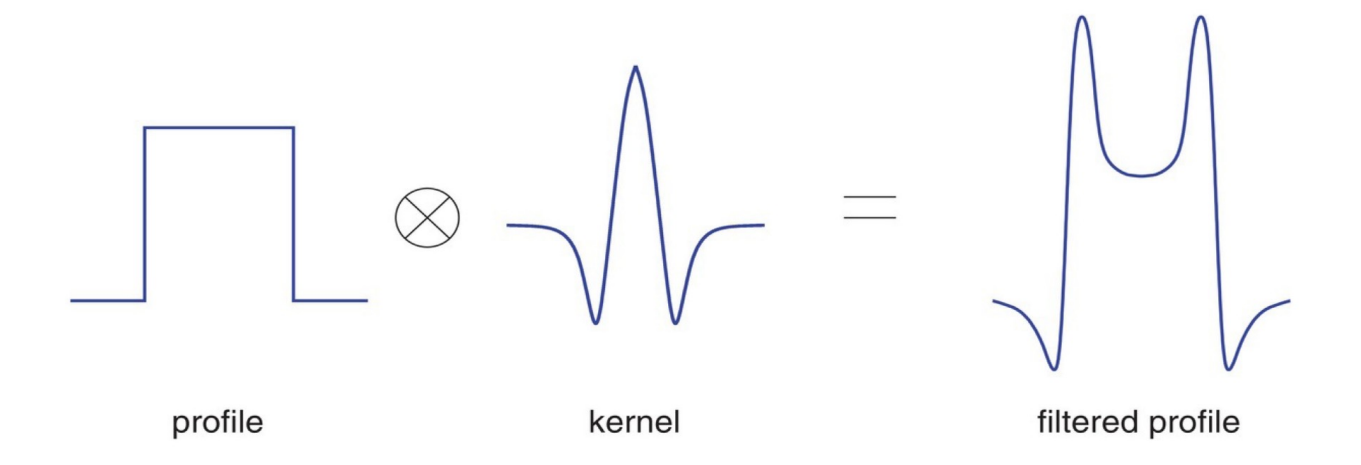
Filtered back-projection

- Reconstruction of tomography from sinograms by filtered back-projection
- In one direction, the radiographic absorption profile is recorded. This projection is then run back through the image, whereby the projection intensity is evenly distributed among all the pixels along each ray path.
- This is then repeated for a set of projection angles spanning 180°, whereby for each angle, the back projection is added to the image. The smaller the angular shift, the more closely the final overlapping set of back-projections resembles the original object

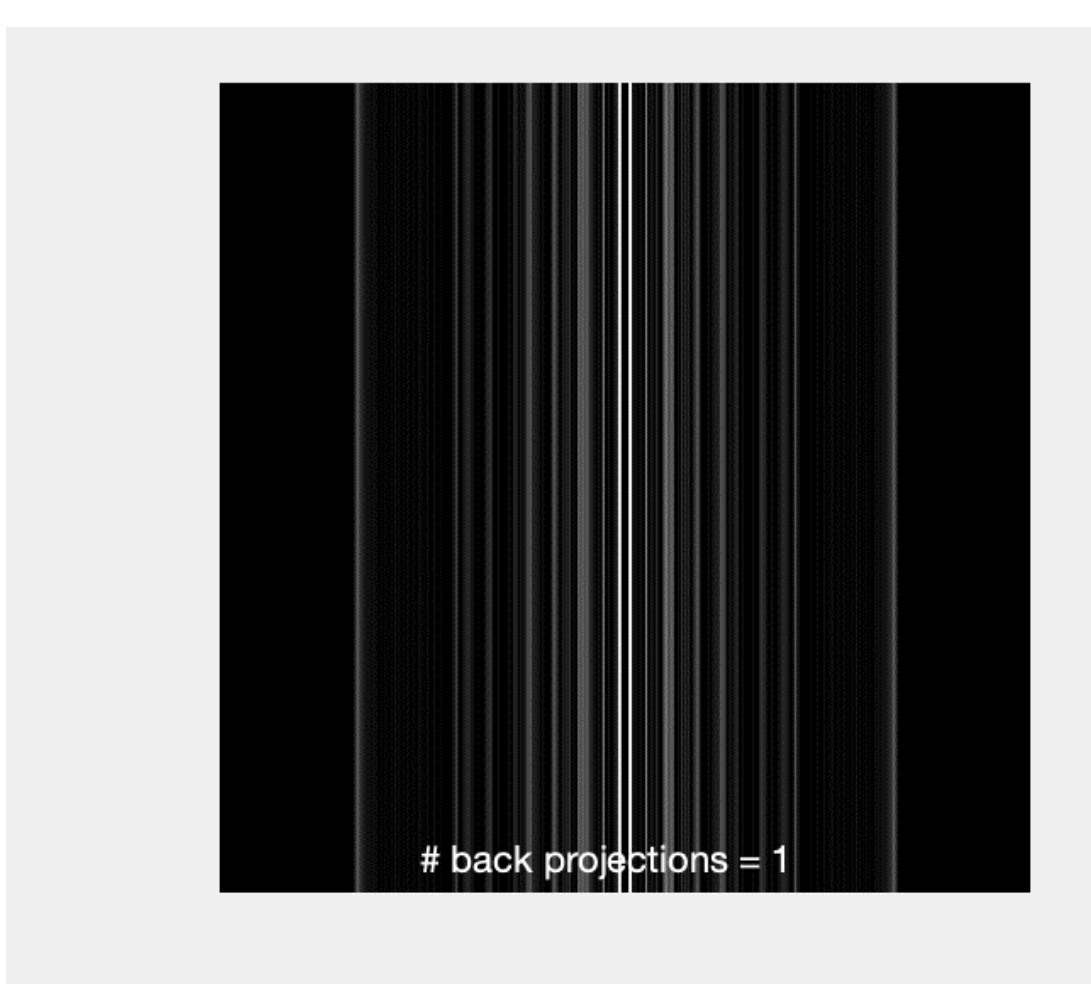


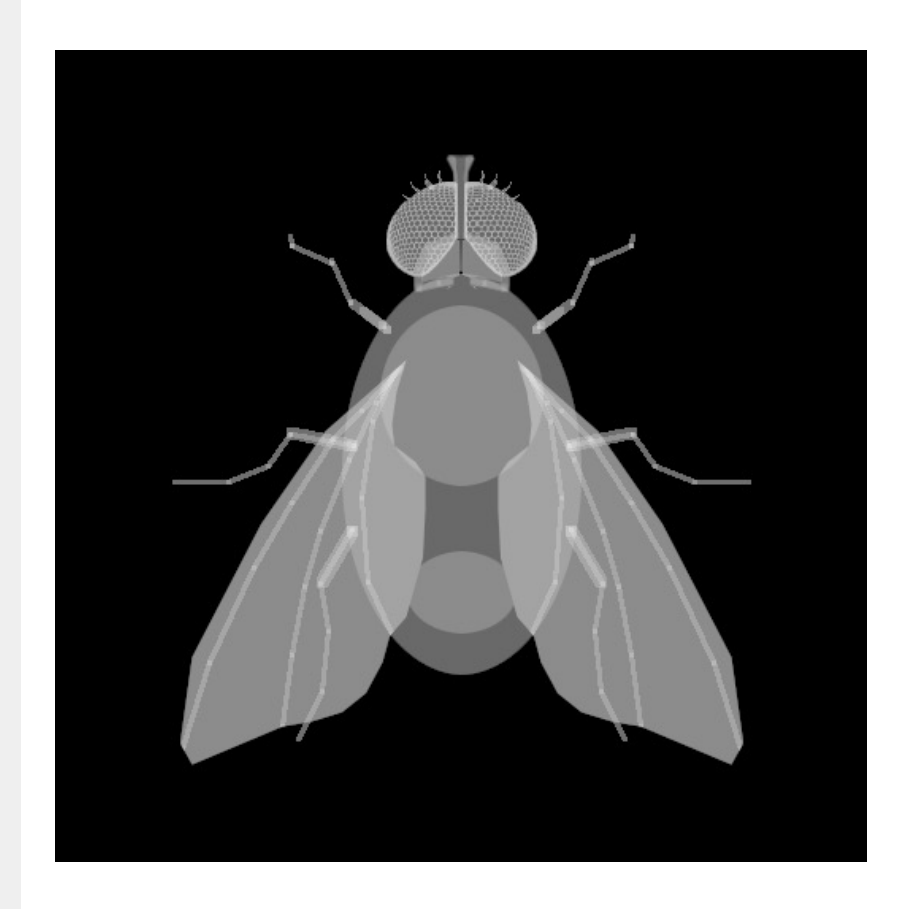
Filtered back-projection

- There is significant distortion due to overlapping projections producing star-like artefacts and a blurring, which becomes increasingly evident near the centre of the reconstruction.
- Lower frequency components tend to be responsible for blurring, while sharper, high-frequency, features might be removed in order to smooth statistical noise.
- These artefacts can be suppressed by careful filtering of the absorption profiles. This is carried out by Fourier analysis – each profile is Fourier-transformed and then treated with a filter, which suppresses certain ranges of the Fourier components.



Filtered back-projection





https://www.synchrotronmovies.com

```
clear all; close all

    vid = VideoWriter('backProjection.mp4','MPEG-4');

    vid.Quality = 100;

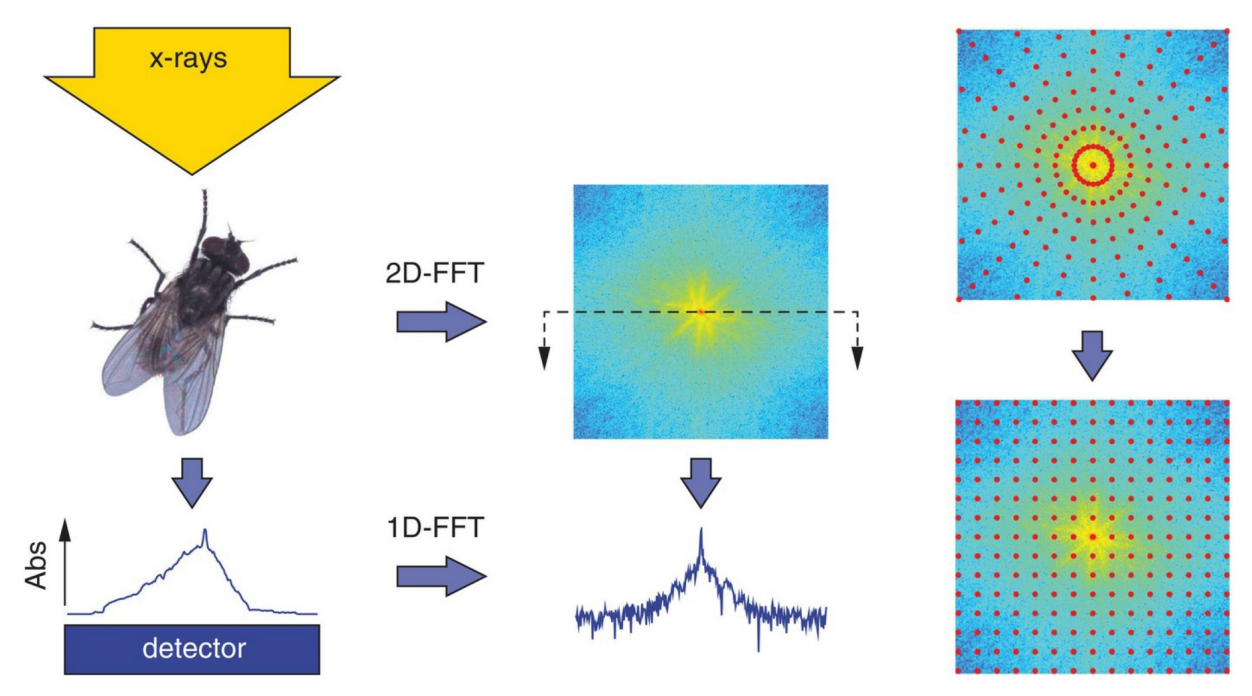
    vid.FrameRate = 10;

    open(vid);

    figure('units','pixels','position',[0 0 1920 1080],'ToolBar','none'); set(0,'defaultfigurecolor',[1 1 1]);
    mylm = imread('cartoonFly.png');
       sino = radon(mylm,0.0000001:180/ii:180); % First one bp only, then 2, 3, etc
       backproj = iradon(sino,0.0000001:180/ii:180);
       imshow(backproi);
       caxis([0 max(max(backproj))]);
       hold on
       axis square
       axis off
       colormap(gray)
      str1 = '# back projections = ';
str2 = num2str(ii, '% 3i');
       strTot = [str1,str2];
       annotation('textbox',[0.32 0.14 0.14 0.07],'String',strTot,'EdgeColor',...
          'none', 'FontSize', 11, 'FitBoxToText', 'on', 'HorizontalAlignment',...
          'left','verticalAlignment','bottom','Color','w');
       frame = getframe(gcf);
       writeVideo(vid,frame);
       if (ii<=10)
         pauseMov(vid,9);
       elseif (ii>10) && (ii<=20)
          pauseMov(vid,4);
       end
       hold off
       delete(findall(gcf,'type','annotation'));
     % Output the movie as an mpg file
    close(vid);
```

Fourier slice theorem

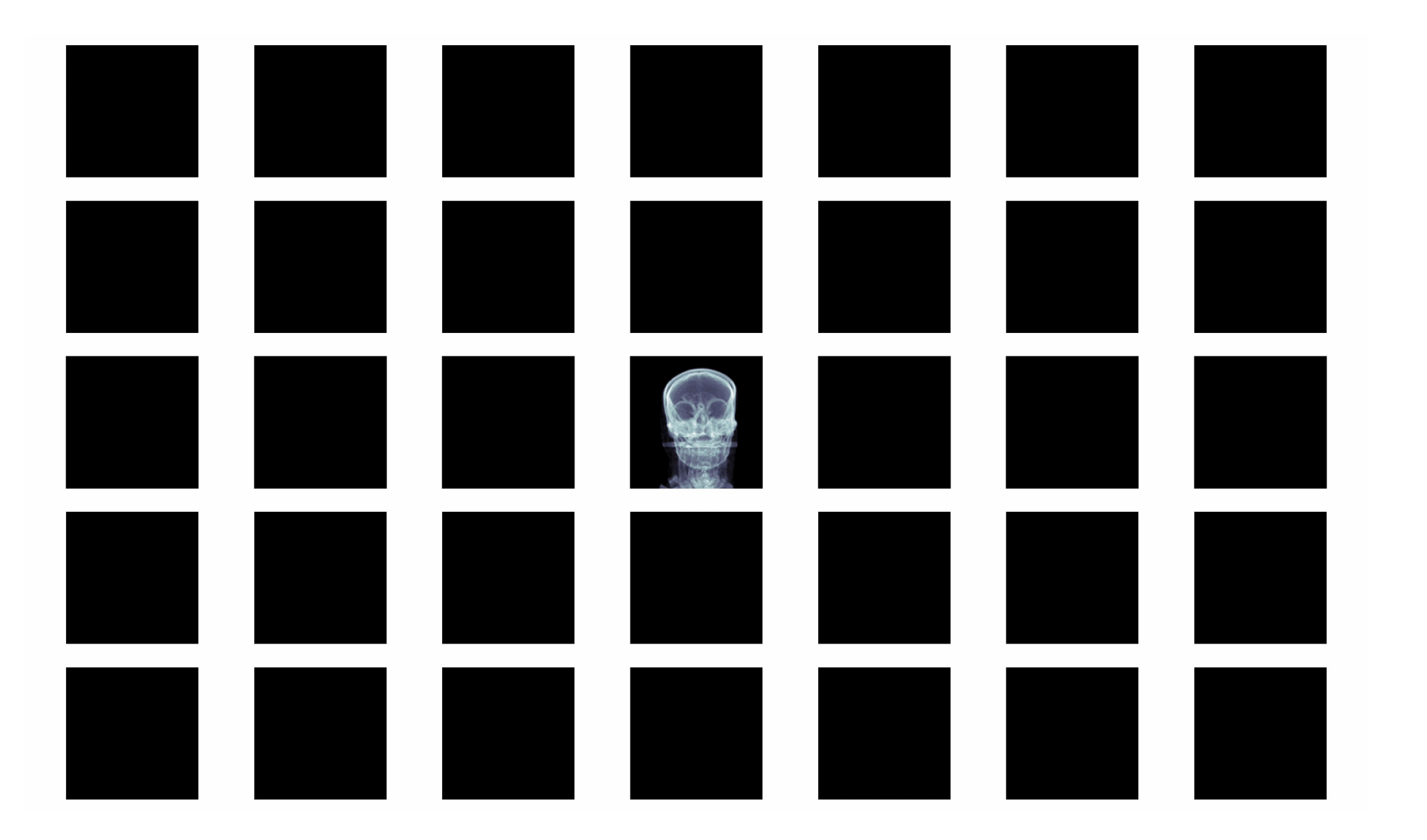
• The one-dimensional Fourier transform of the projection of a two-dimensional object (i.e. a slice) onto a line (i.e. the transmission profile at the height of the slice) is equal to the one-dimensional slice through the centre of the two-dimensional Fourier transform of the same object.



Fourier slice theorem

- By Fourier transforming in one dimension a given projection, we obtain a line in the 2D-Fourier transform of the object.
- By collecting all the projections between 0 and 180° (the sinogram), we fill the entire Fourier-space representation of the object.
- The tomogram is obtained by a reverse FT.

The final three-dimensional reconstruction consists of a stack of all the
reconstructed tomograms. The resolution of the reconstruction is determined by the
dimensions of voxels, or resolution elements. Tomographic images comprise an array
of these voxels on a regular three-dimensional grid, whereby each voxel is
associated with a certain physical value, such as the average linear absorption
coefficient within that voxel, or the phase shift induced by the voxel



Practial considerations

- Dark noise and flat corrections
- Drift + eccentricity of rotation axis
- Beam hardening
 - Pink beam is not perfectly homogeneous: more higher energies near the center
 - Shape of the energy spectrum shift while passing through the sample
 - Manifests itself as an apparent decrease in attenuation in the center

Contrast for weakly interaction matter

The contrast in an absorption radiograph between two points A and B is defined as being

$$C_a = \frac{I_A - I_B}{I_A}$$

where IA > IB. For an equal distance z passed through the sample to produce the intensities at A and B, we have

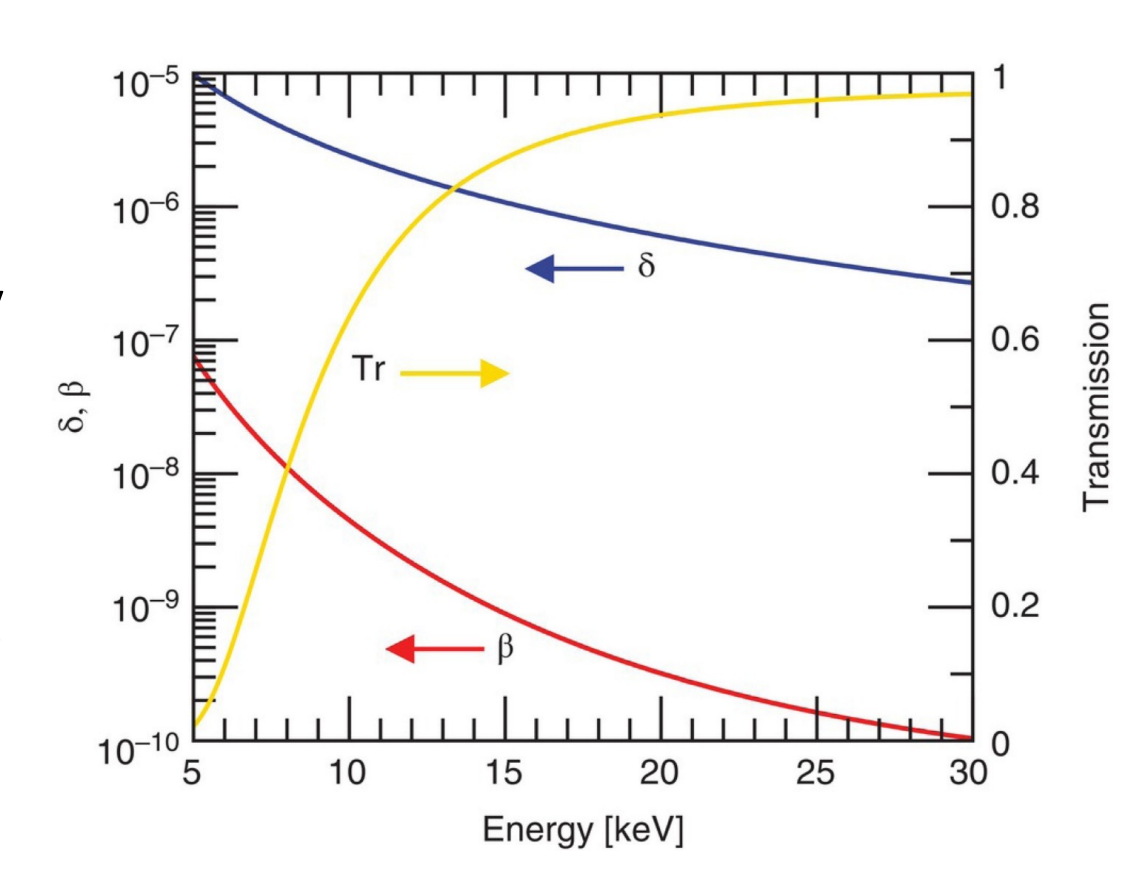
$$C_a = \frac{\exp(-\mu_A z) - \exp(-\mu_B z)}{\exp(-\mu_A z)}$$
$$= 1 - \exp[(\mu_A - \mu_B)z].$$

For weakly absorbing materials with similar attenuation coefficients ($\mu Az \sim \mu Bz \ll 1$), this is approximated by

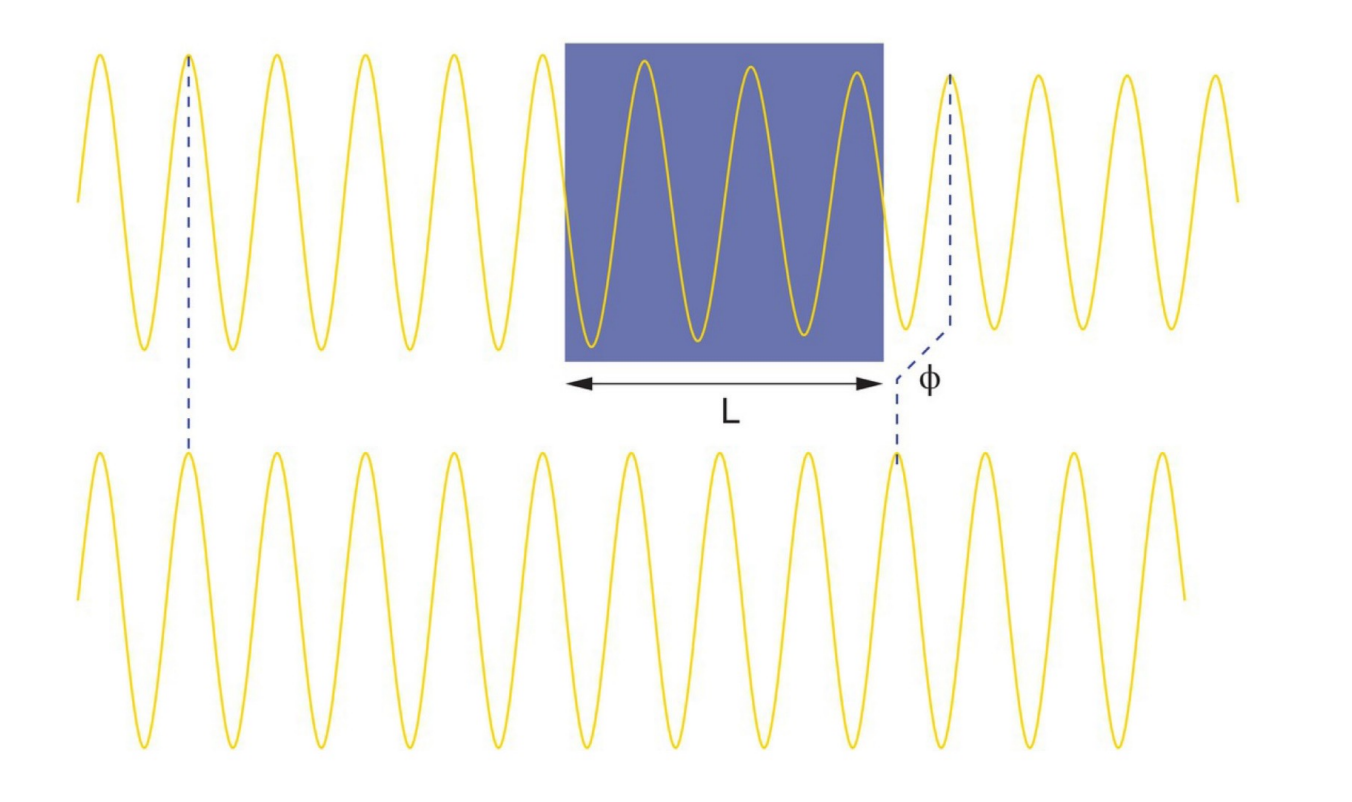
$$C_a = (\mu_B - \mu_A)z$$

Consider fat (mass density 0.9 g cm⁻³) and muscle (1.06 g cm⁻³), probed using 20 keV (0.62 Å) radiation. At this energy, the absorption coefficients of fat and muscle are, respectively, $\mu_f = 5.3 \times 10-5 \ \mu m^{-1}$ and $\mu_m = 6.2 \times 10-5 \ \mu m^{-1}$. The contrast is therefore $9 \times 10^{-6}z$, whereby z is in microns. So, for example, for z = 1 mm, the contrast remains less than 1%.

- Absorption contrast can be low for elements with similar electron density, in particular for light materials.
- Absorption falls off much more steeply with energy than do refraction effects. This is most pronounced for lighter elements, as β scales as Z^4 , while δ is approximately proportional to Z.
- Exploiting fluctuations in δ can thus be used to advantage in so-called phase-contrast imaging techniques

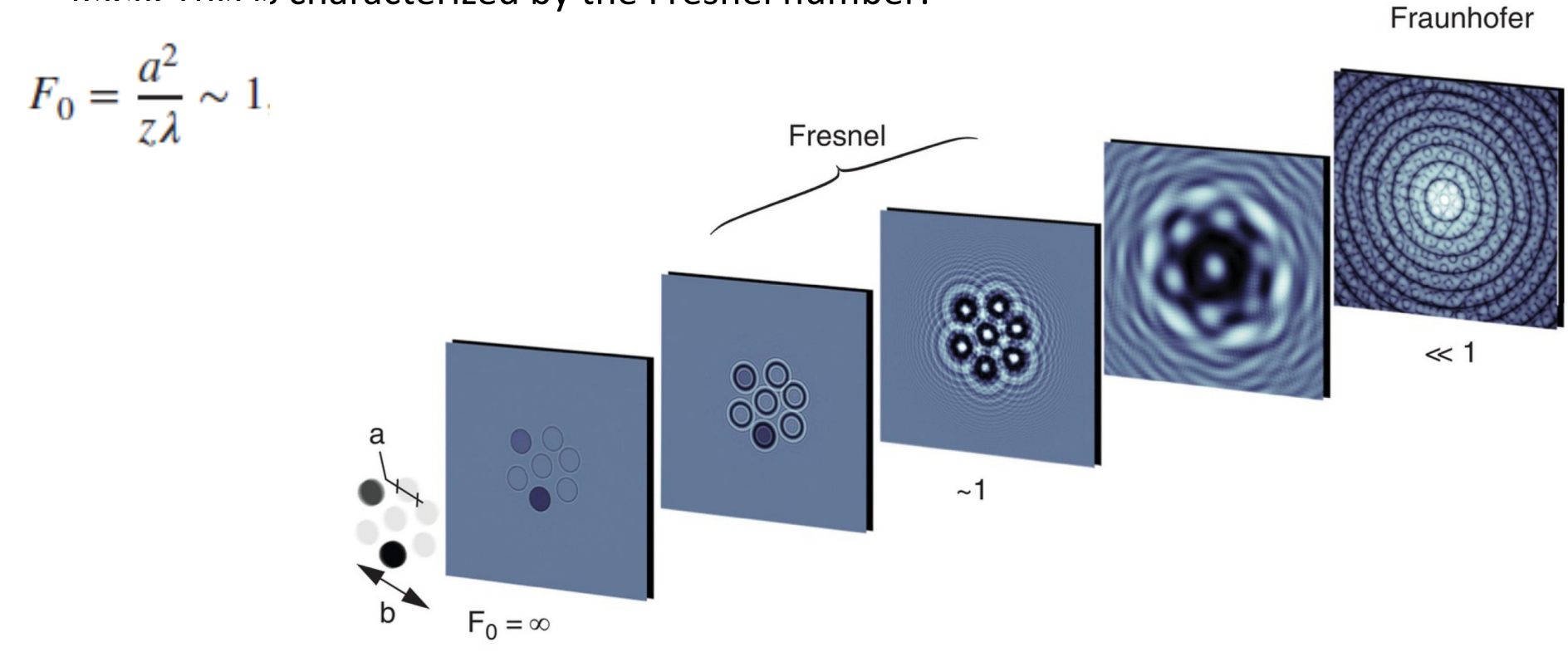


• Two parallel x-ray beams which are initially in phase become out of phase by an amount φ .

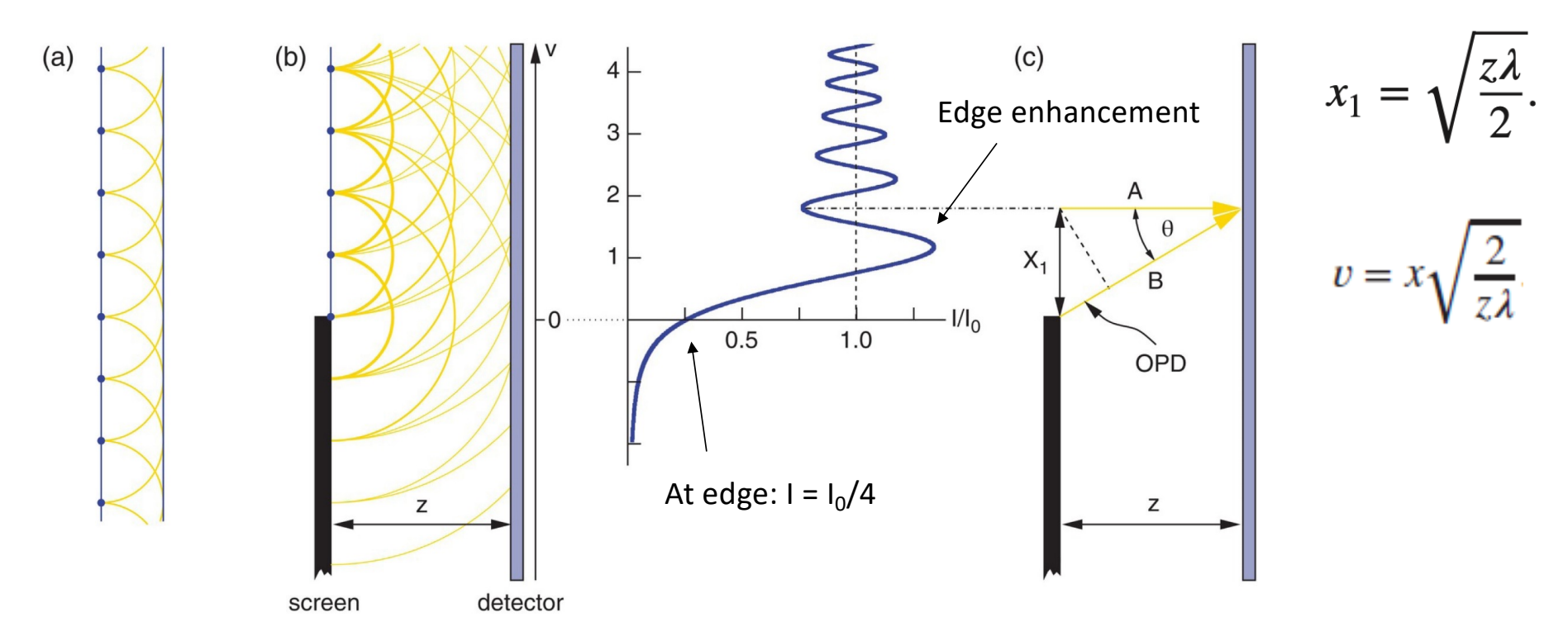


$$\phi = \frac{2\pi L\delta}{\lambda}$$

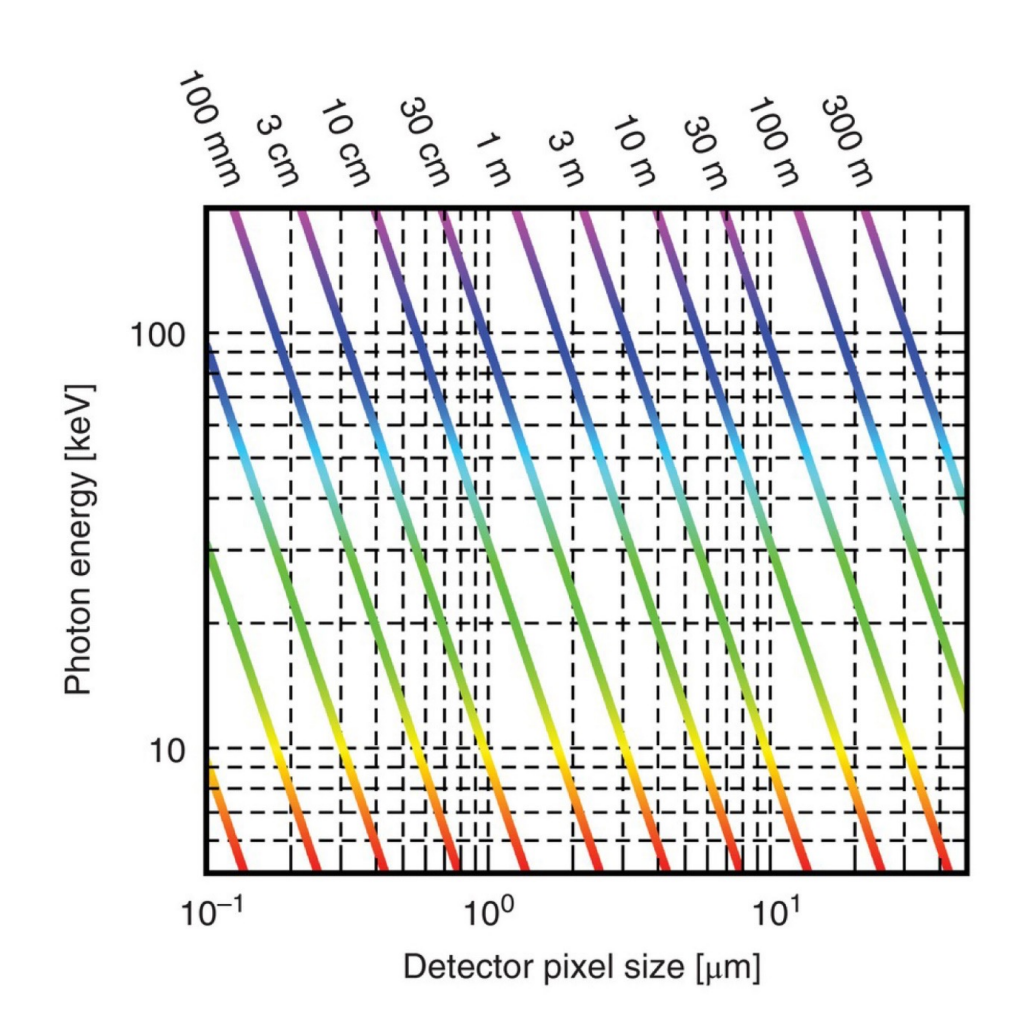
 Fresnel-diffraction regime extends until the diffraction features (fringes) are separated by a distance similar to the linear dimensions of the scattering object itself. This is characterized by the Fresnel number:



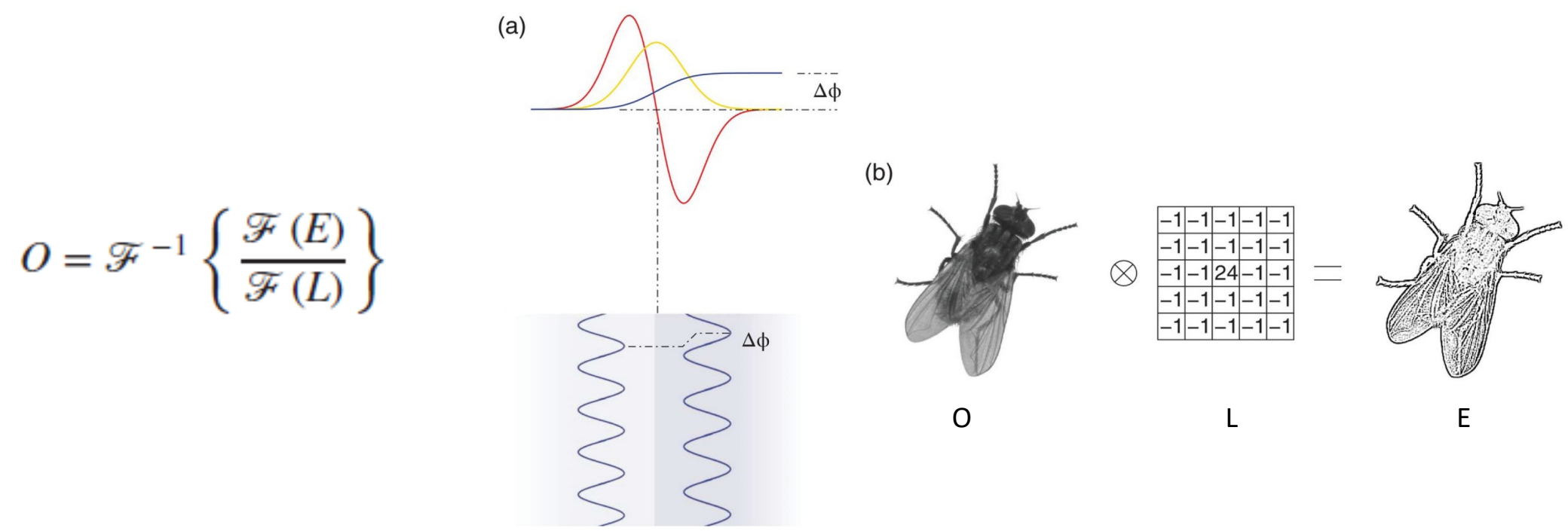
• The pattern on a detector at a distance z from a parallel beam of x-rays partially blocked by an opaque screen exhibits interference fringes in the region close to the projection of the edge of the screen

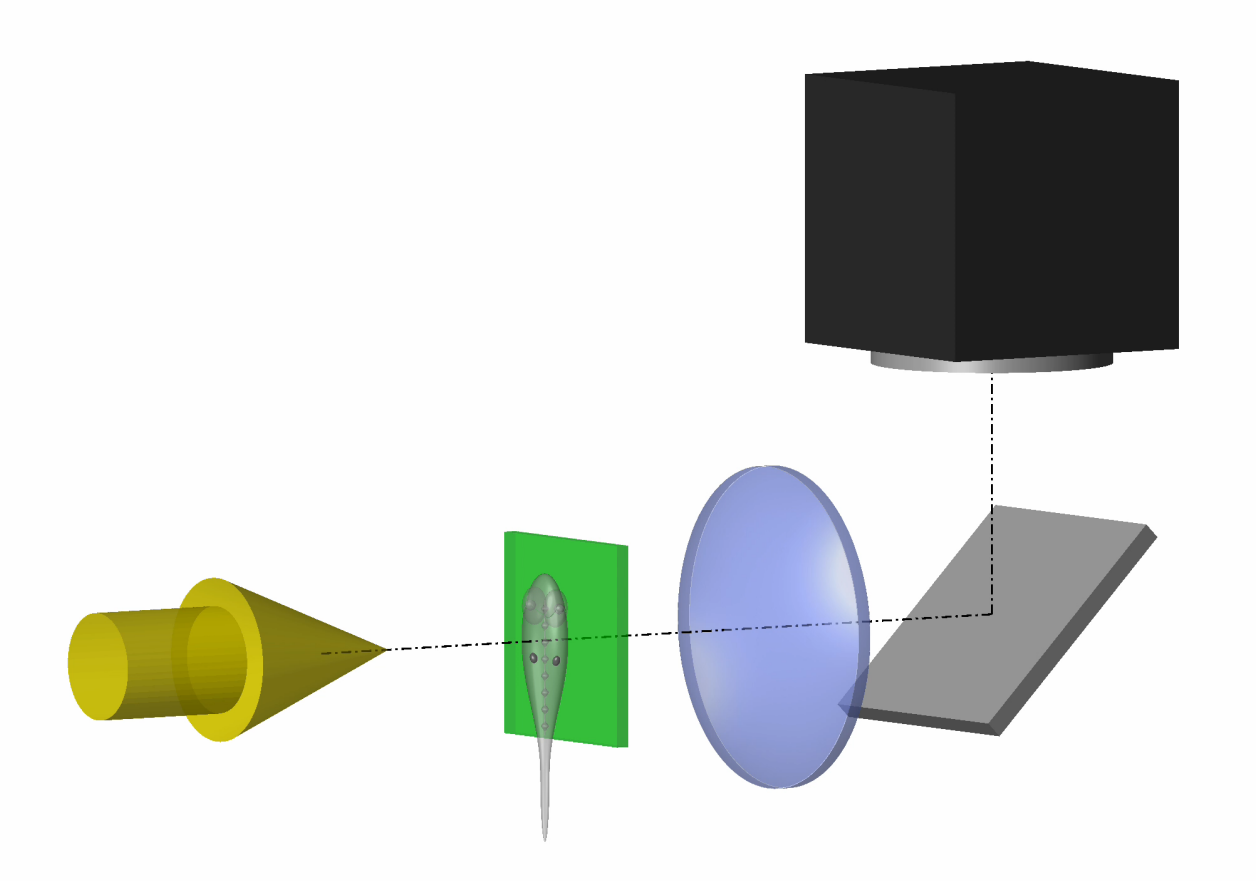


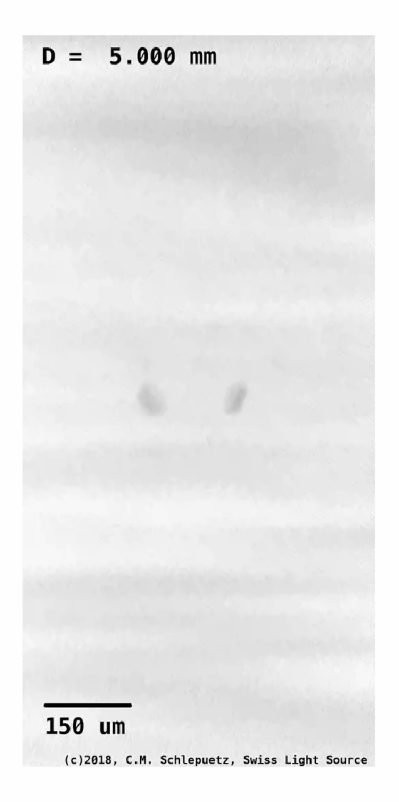
- Edge enhancement is used in tomography to highlight internal and external boundaries of heterogeneous samples for which the absorption coefficients of the component parts are similar
- The sample–detector distance Z_0 should be in the Fresnel regime at $F_0 \sim 1$, adjusted so that the lateral resolution (pixel size, Δ) matches this fringe separation: $Z_0 = (2\Delta)^2/\lambda$



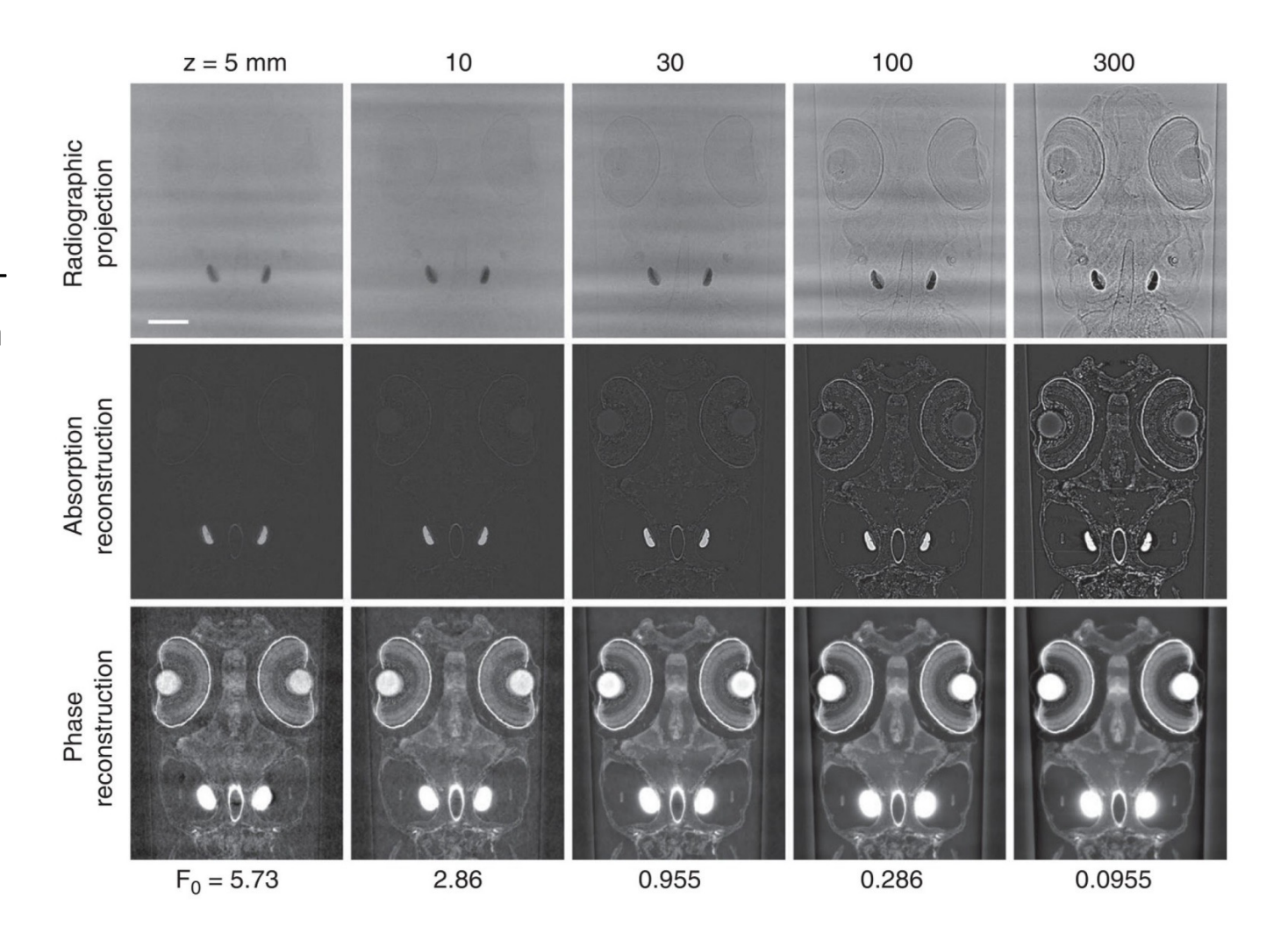
• Refraction and interference result in a modulation in the intensity in the Fresnel regime at the geometric projection of the boundary between two parts of a phase which induce different relative phases – this fringe profile can be approximated by a function of the form $x \exp(-x^2/2\sigma^2)$







Propagation-based tomography of a zebrafish embryo recorded using 21 keV x-rays and a detector with a pixel size of Δ = 0.65 μ m.



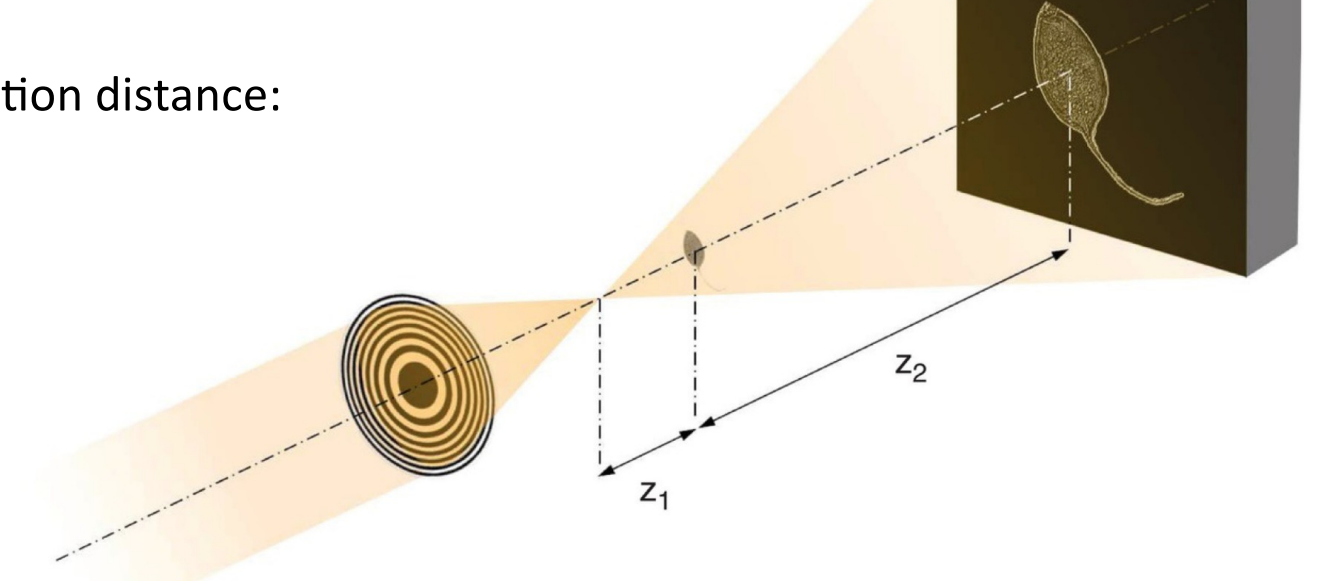
Zoom tomography

- The sample is placed downstream from the focal point of a focussed beam
- Resolutions of a few tens of nm are routinely achievable
- Magnification depends on ratio z₁ and z₂

$$M = \frac{z_1 + z_2}{z_1}$$

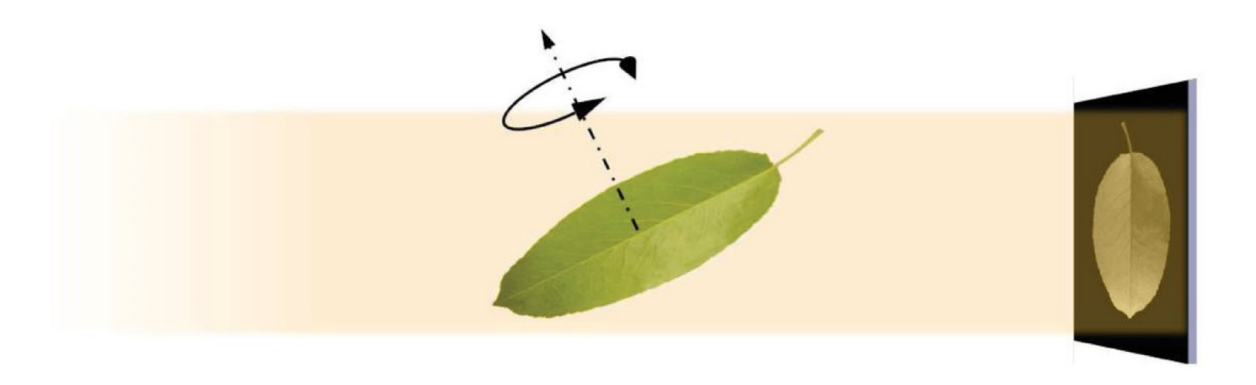
• Equivalent propagation distance:

$$z = \frac{z_1 z_2}{z_1 + z_2}$$



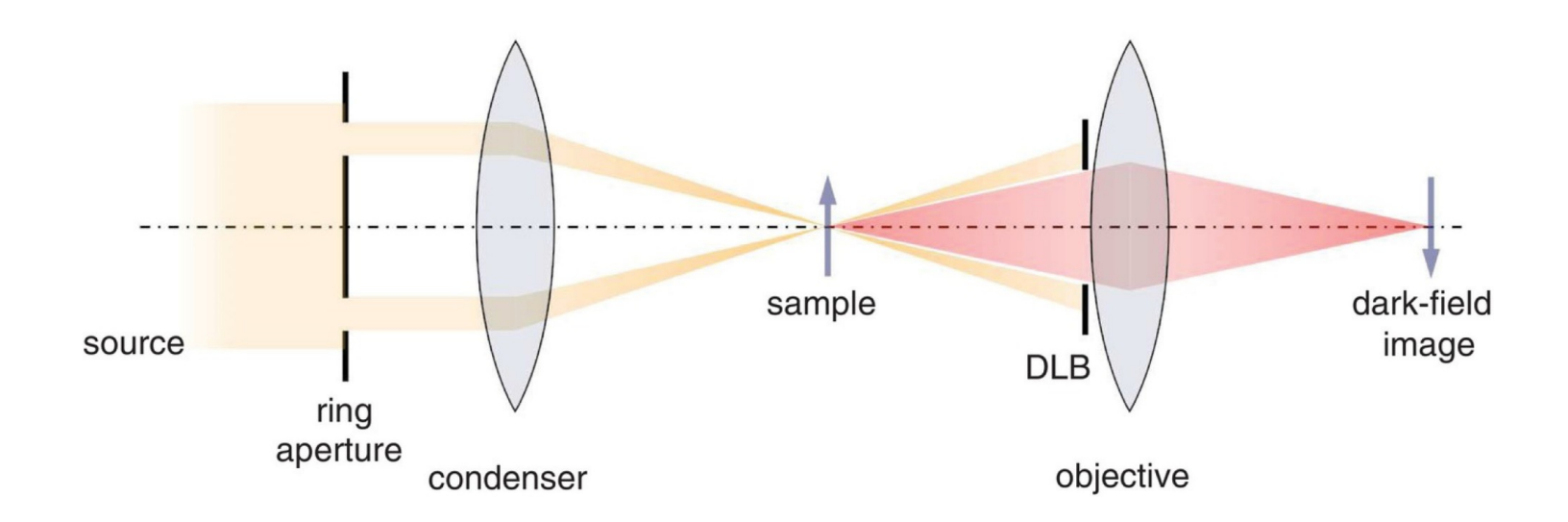
Laminography

- Laminography is a special configuration of tomography used for large flat samples
- The sample is tilted so its rotation axis (set to be perpendicular to the large, flat, facet of the sample) is neither parallel nor perpendicular to the incident beam



Dark field microscopy

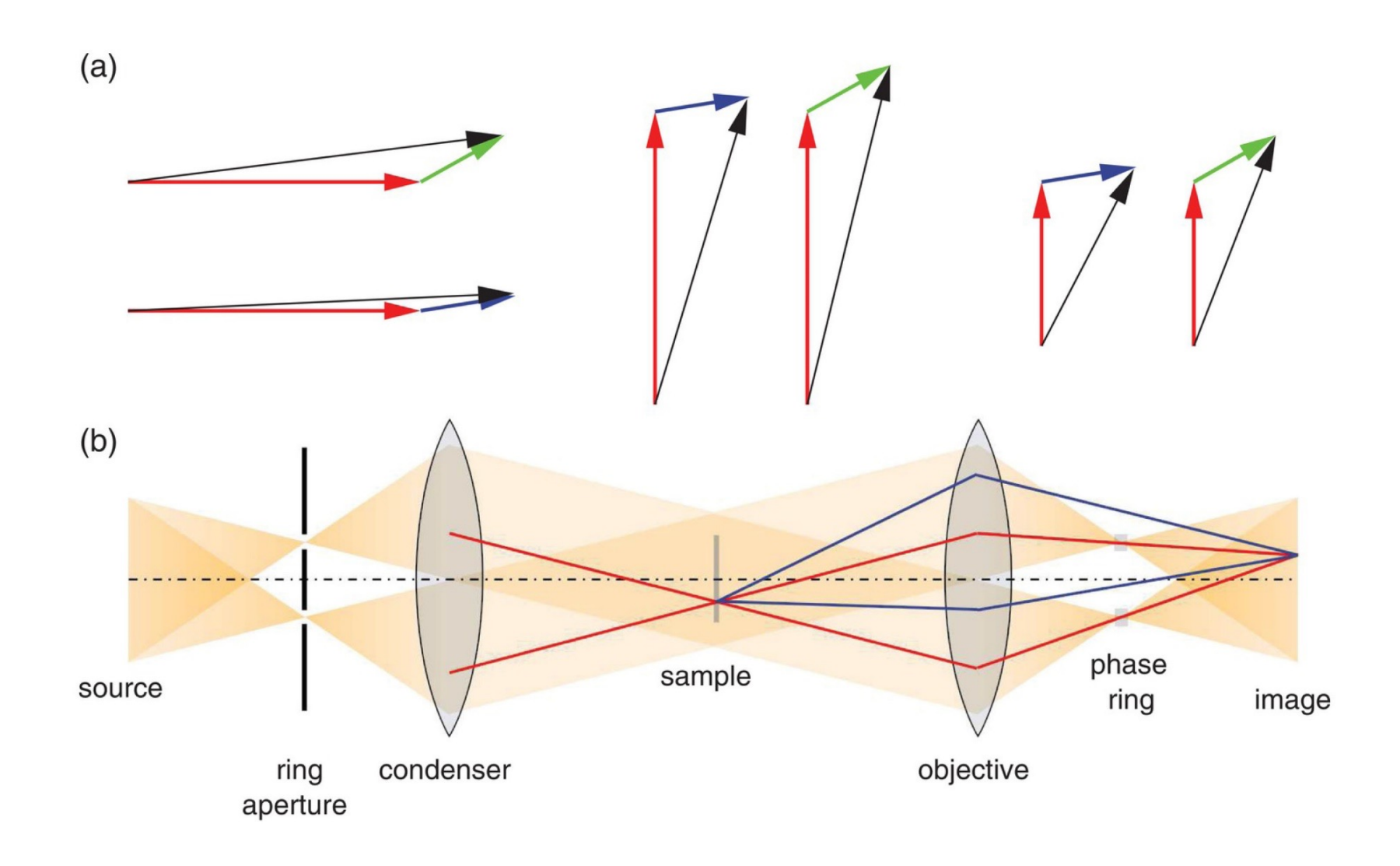
- The direct, undeviated beam after sample illumination is blocked, and only the scattered signal is collected
- Especially useful in highlighting small, dense features (which scatter strongly) embedded in a large object.
- Insensitive to phase variations, as there is no reference wave



Zernike X-ray Microscopy

- Frits Zernike received the Nobel Prize in Physics in 1953 for his invention of phasecontrast microscopy
- Convert phase shifts in radiation scattered from a sample to intensity changes, by vectorially adding the scattered wave vectors to a reference vector. The amplitude of this summed vector changes, according to the relative phase between the reference and scattered waves.
- For a weakly absorbing object the unperturbed fraction of the beam dominates the signal intensity
- Trick: induce a significant phase shift in the reference beam

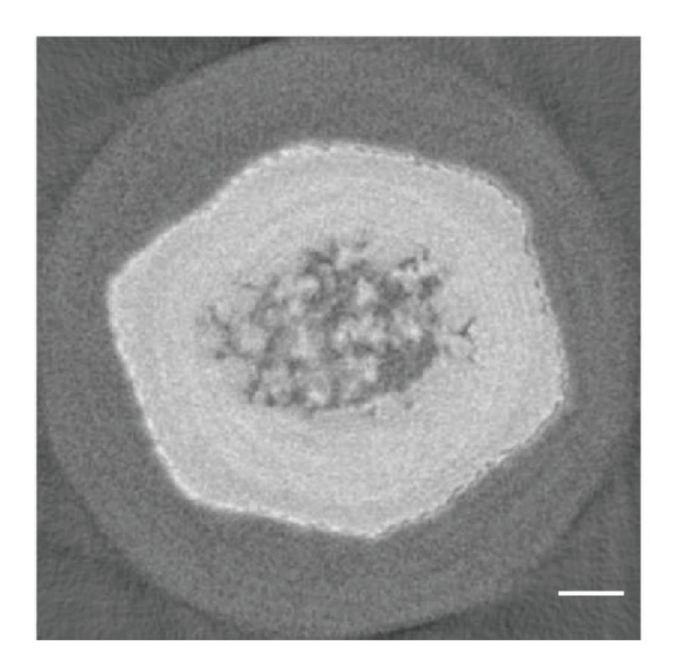
Zernike X-ray Microscopy



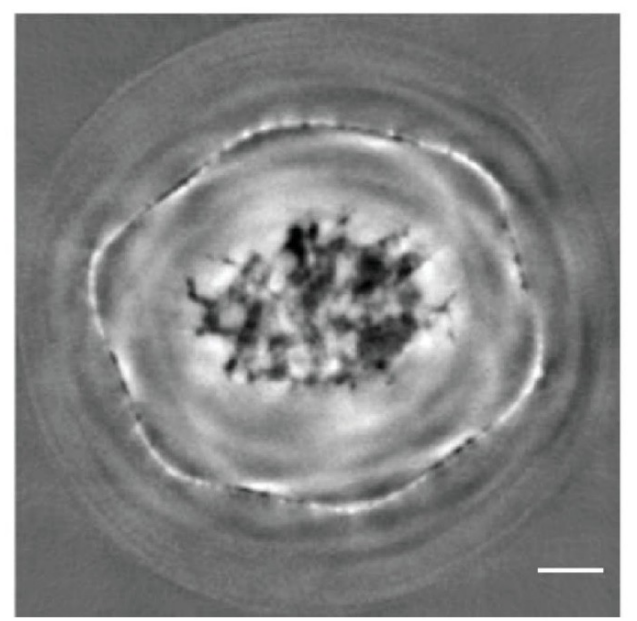
Zernike X-ray Microscopy

• Example: Zernike microscopy of a Nb₃Sn superconductor filament

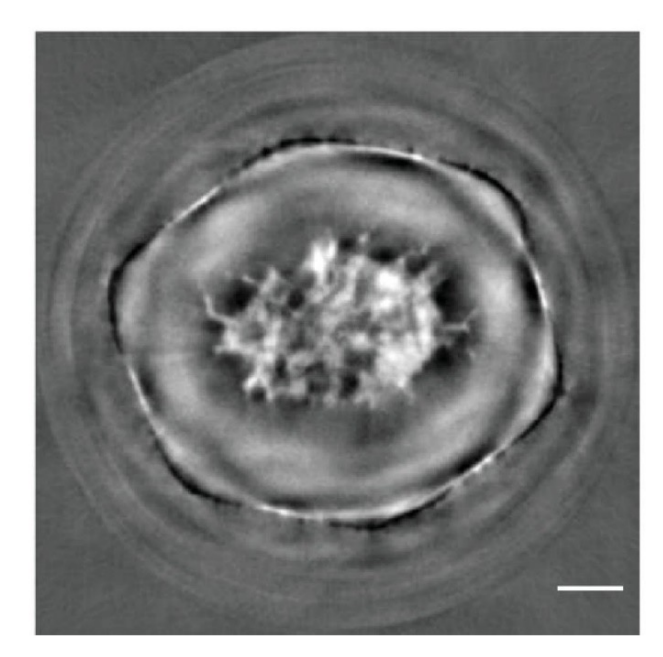
absorption mode



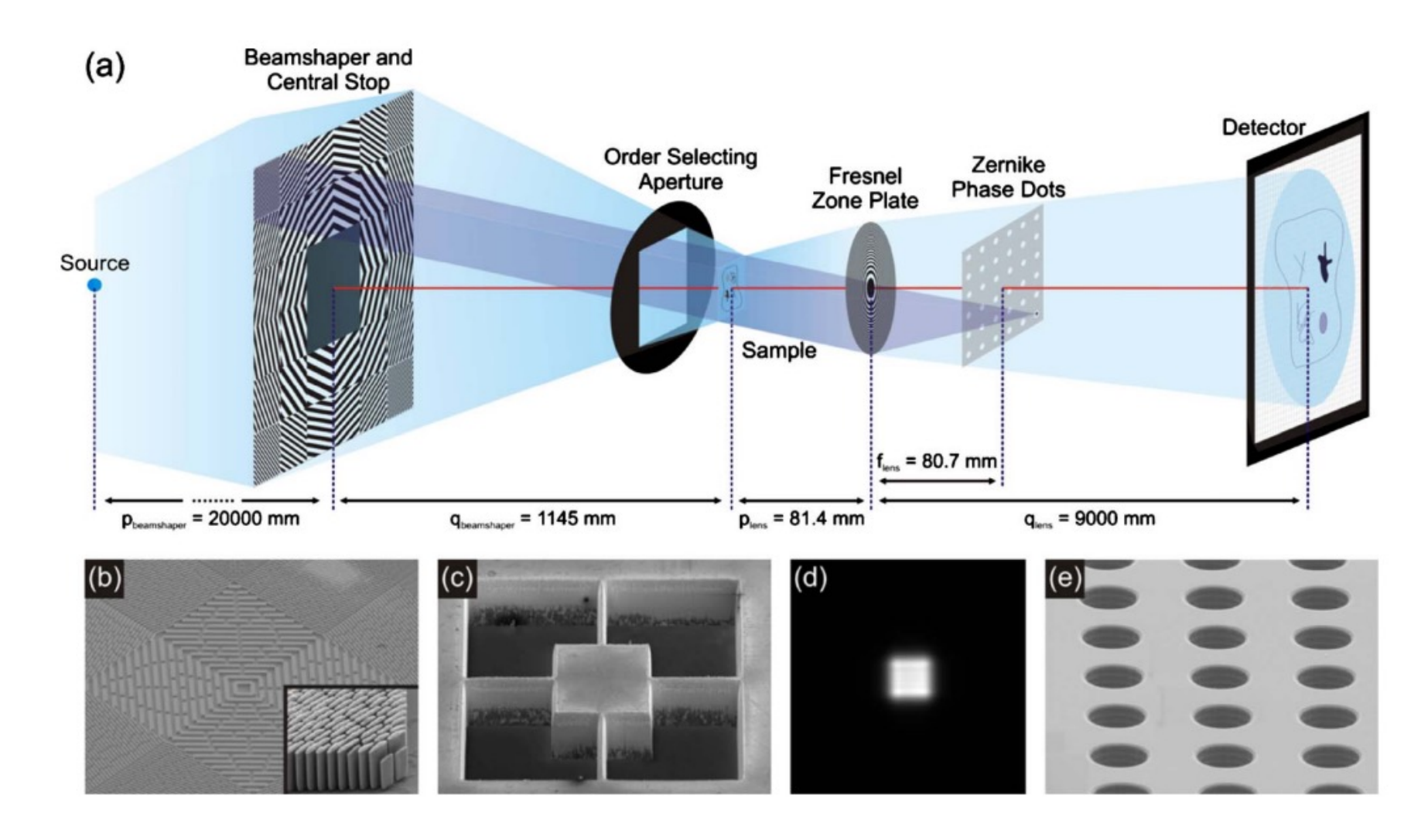
positive-phase ($\Phi = \pi/2$) contrast



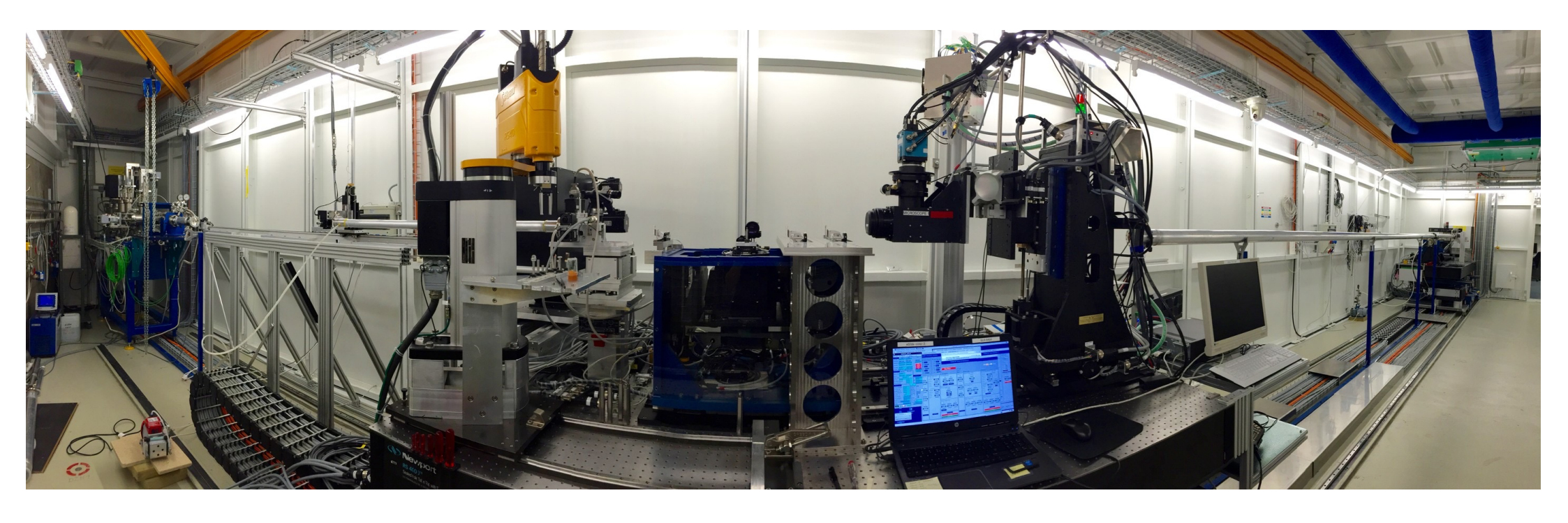
negative-phase ($\Phi = 3\pi/2$) contrast



Nanoscope @ TOMCAT



Nanoscope at TOMCAT



The detector, placed downstream about 10 m, records the magnified phase contrast image of the sample. The field-of-view is from about $75\mu m^2$.

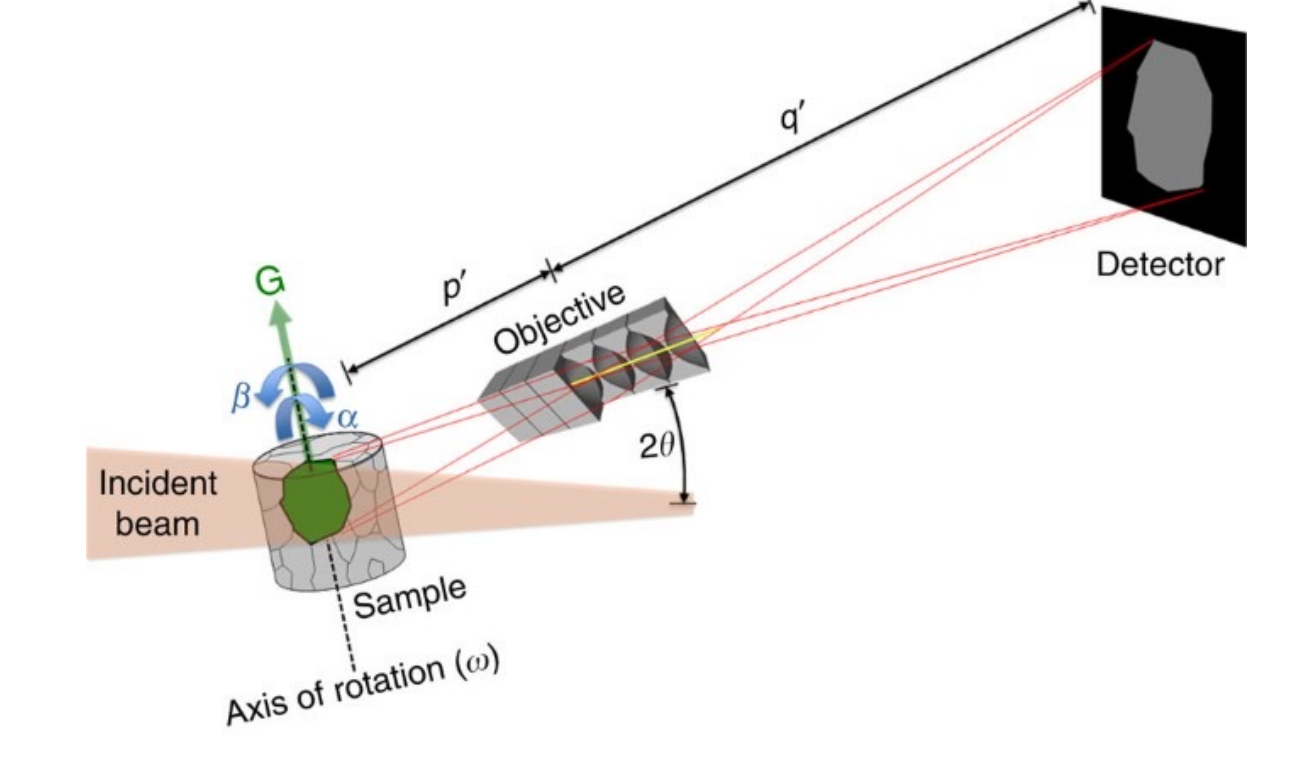
Pixel size down to 65nm (approximately 150/200 nm spatial resolution)

Dark-field X-ray microscopy

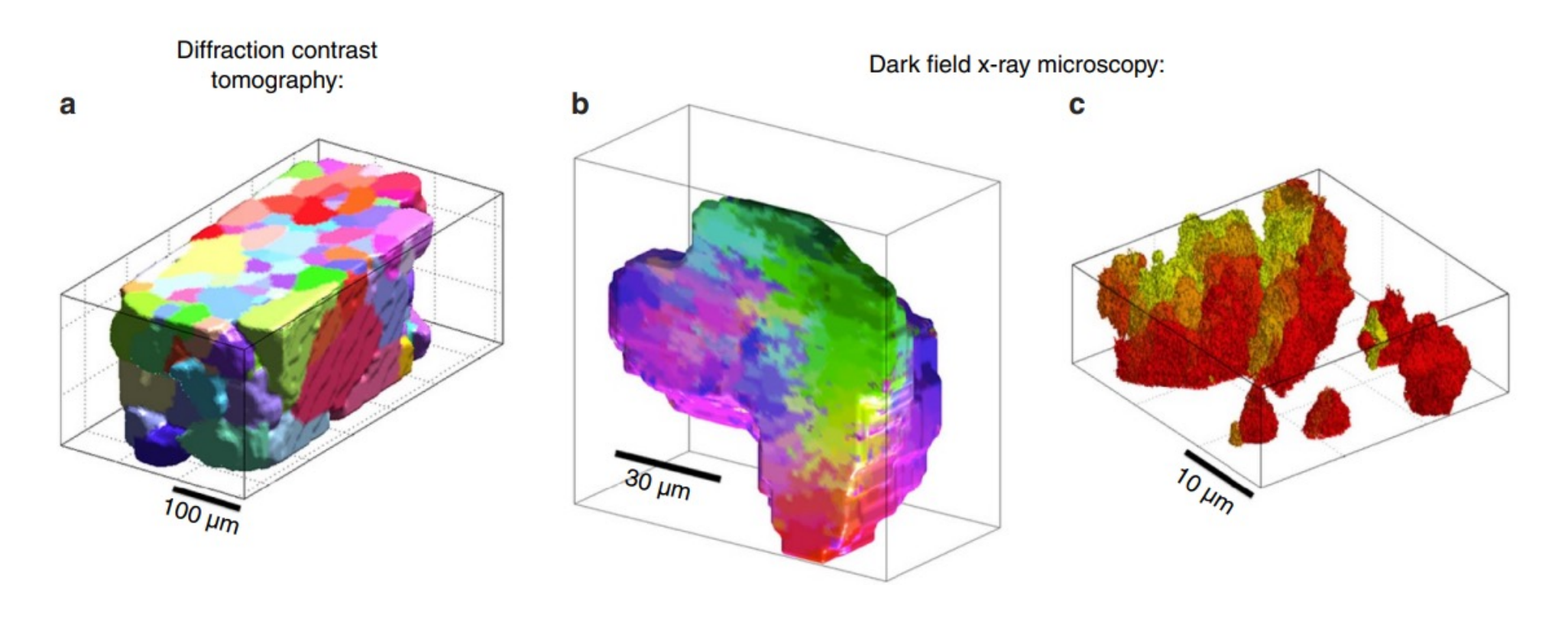
The objective magnifies the diffracted beam by a factor M = q'/p' and generates an inverted 2D projection of the grain. Through repeated exposures during a 360° rotation of the element around an axis parallel to the diffraction vector, G, several 2D projections of the grain are

obtained from various angles.

A 3D map is then obtained by combining these projections using reconstruction algorithms similar to those developed for CT scanning.

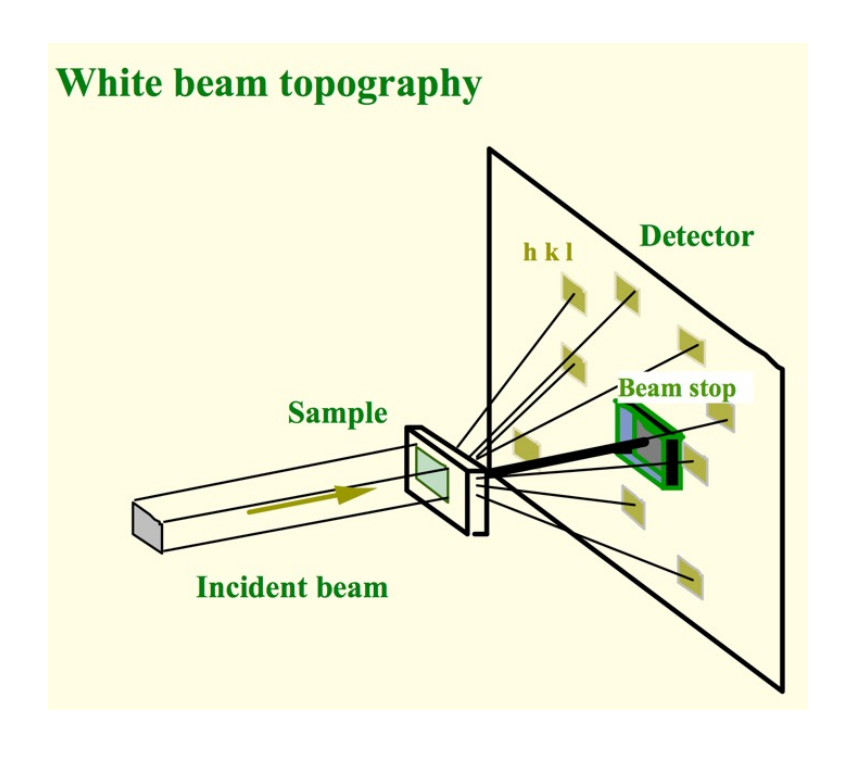


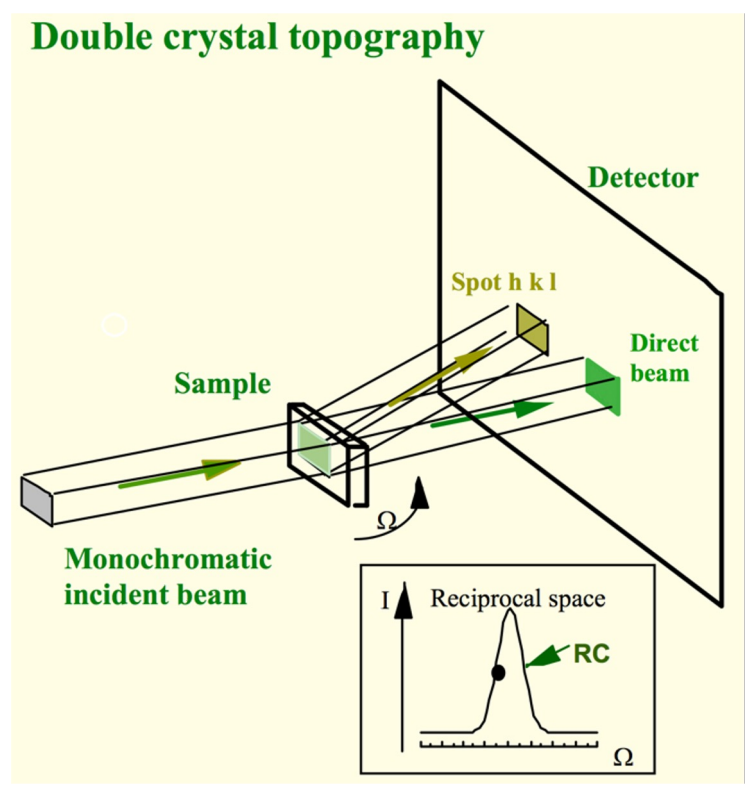
Dark-field X-ray microscopy



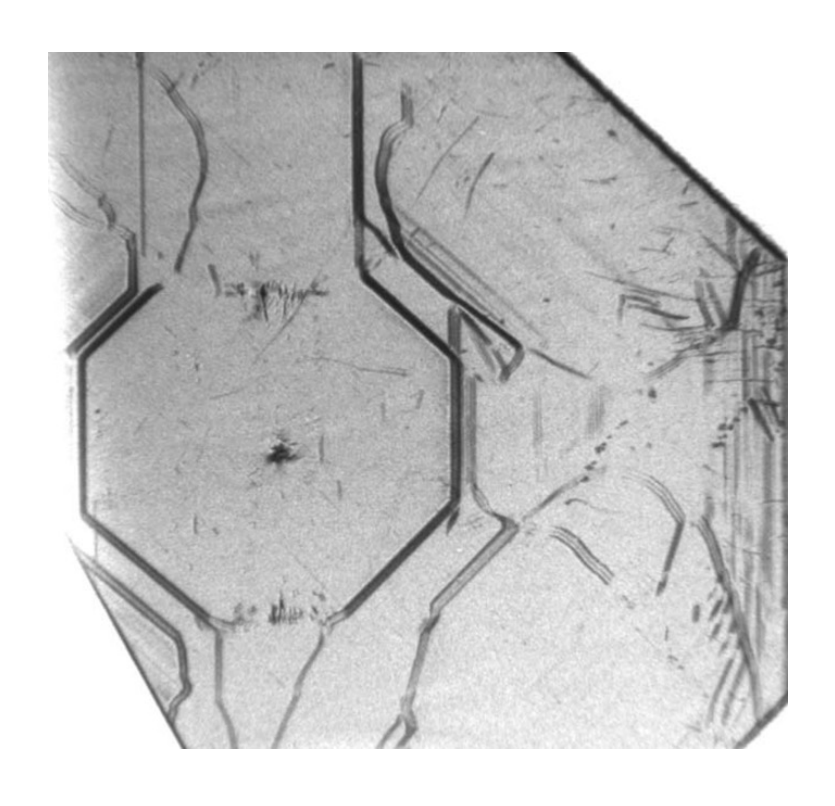
The spatial resolution from left to right is 3.5 μ m, 1.5 μ m and 300 nm, and the angular resolution is 0.5°, 0.15° and 0.03°, respectively.

X-ray topography





X-ray topography

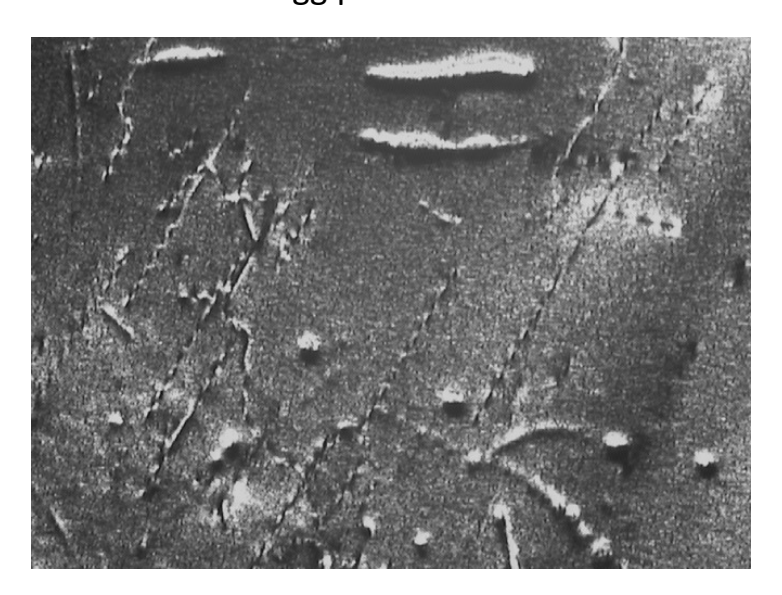


Images José Baruchel



X-ray topography

Bragg peak maximum



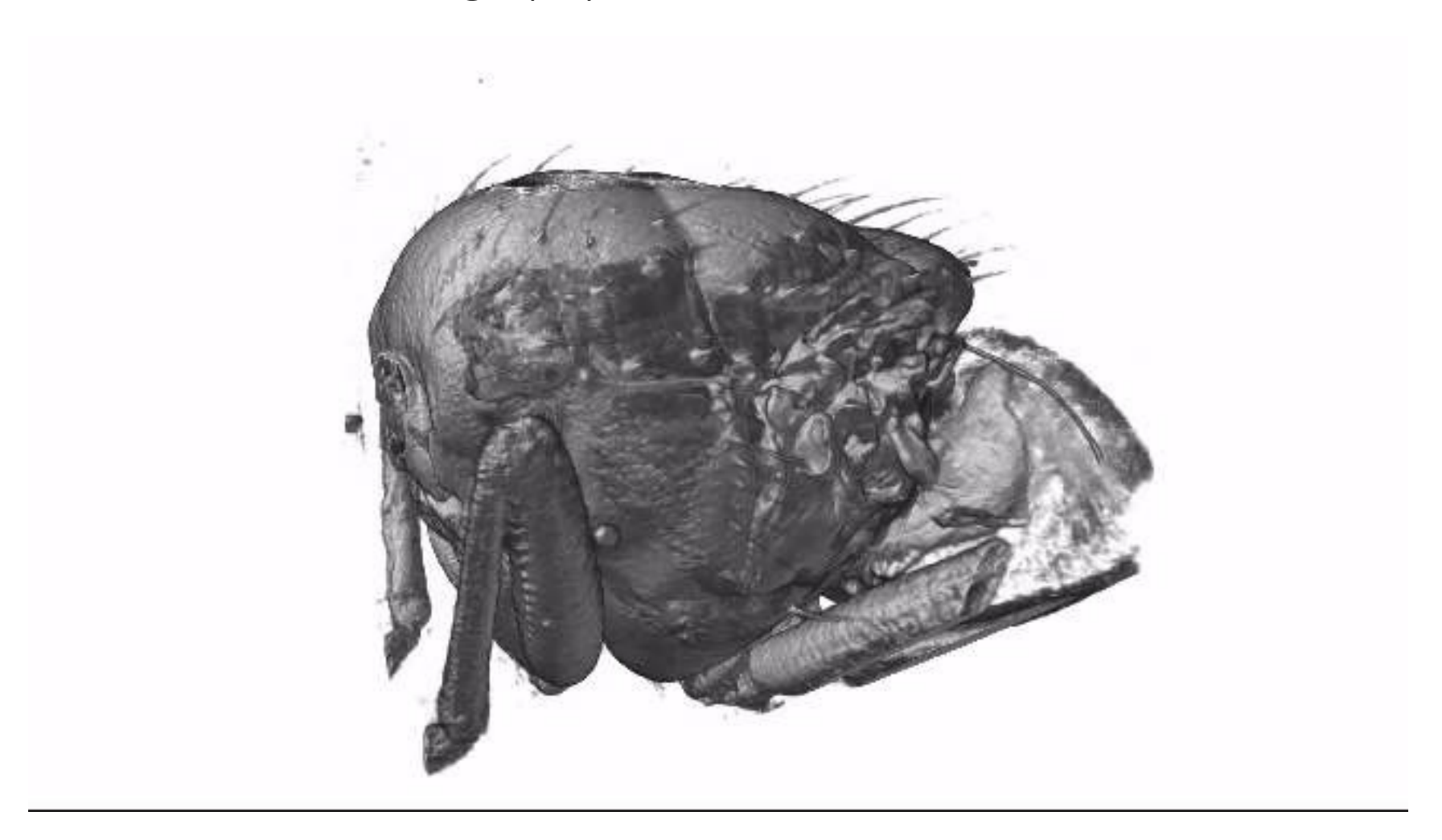
Weak beam conditions



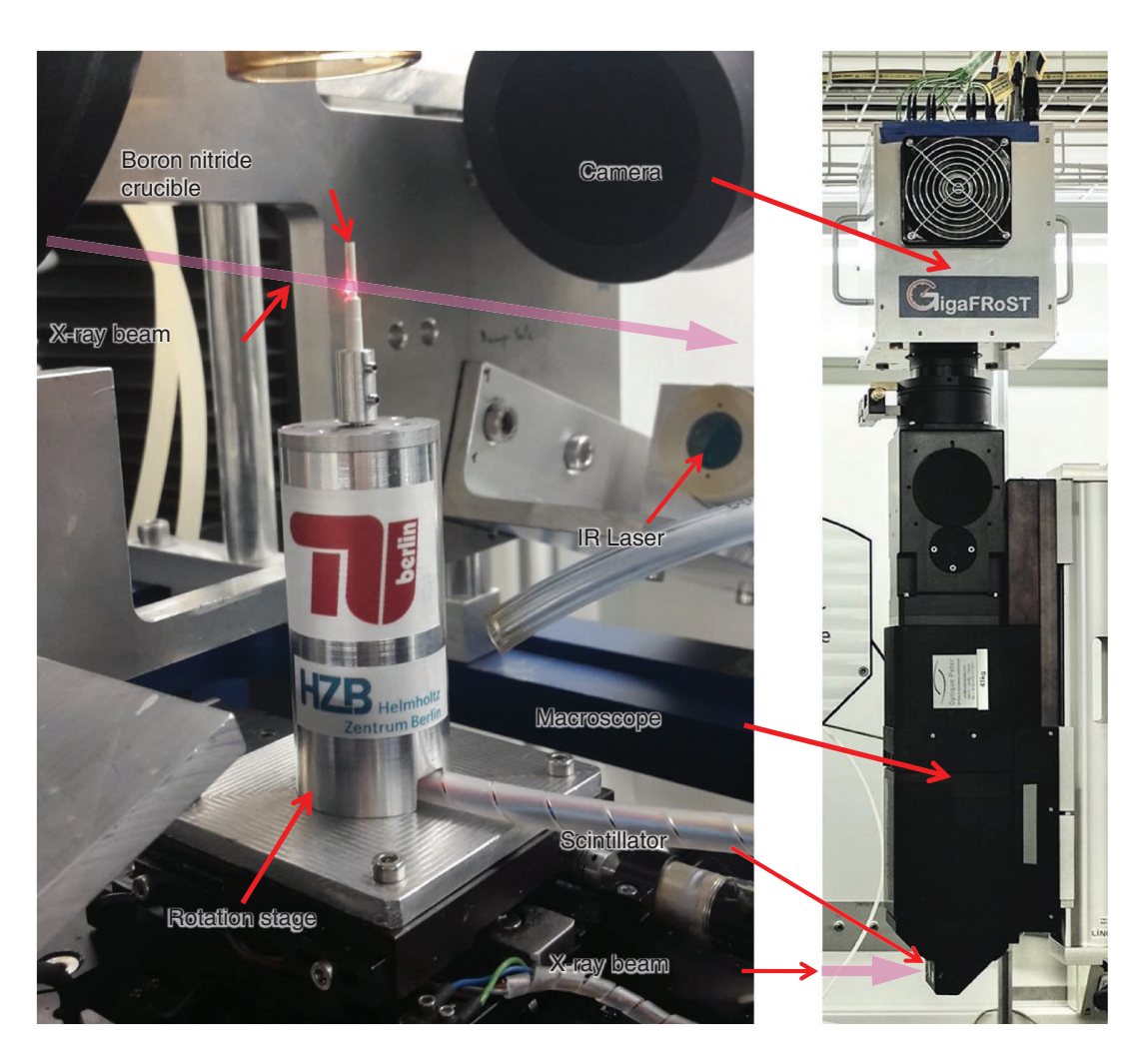
What about time resolution?

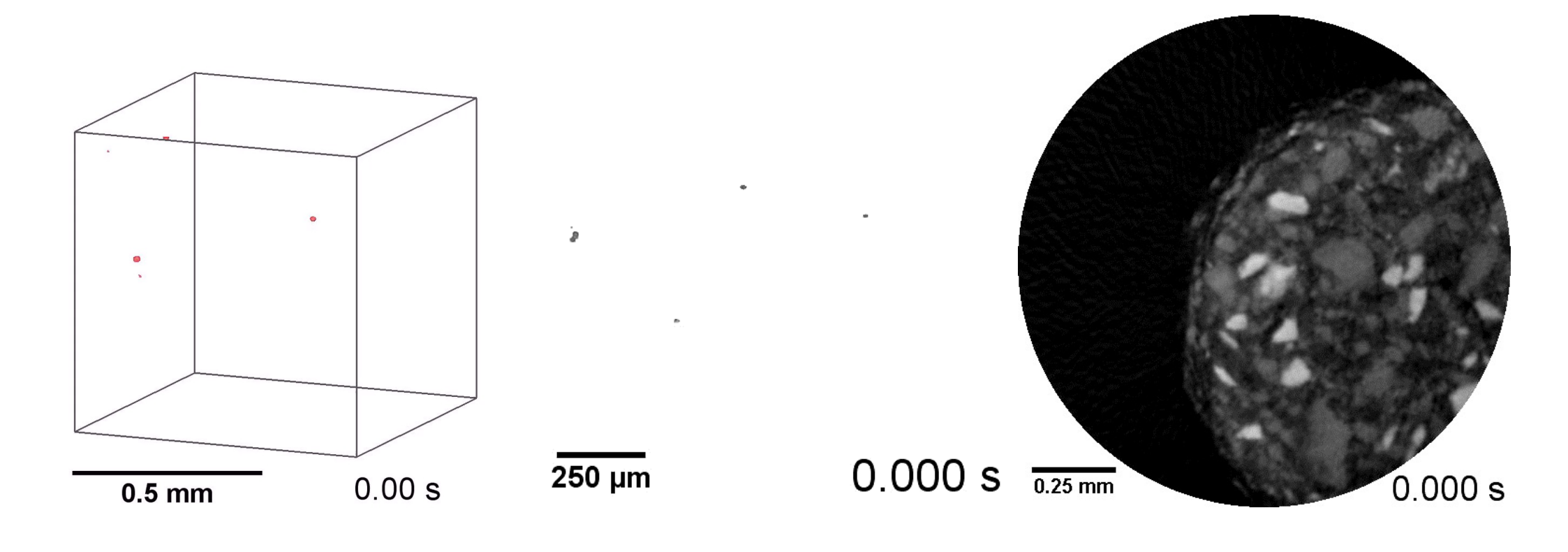
- Factors to consider:
 - the brilliance of the x-ray beam
 - the detector performance (sensitivity and readout time)
 - accurate synchronization of sample position and exposure time
 - the effects of centrifugal distortion of the sample
- If a process is repeatable with a spatial reproducibility equal to or superior than the desired resolution, a stroboscopic approach is possible.

Fast tomography



Fast tomography

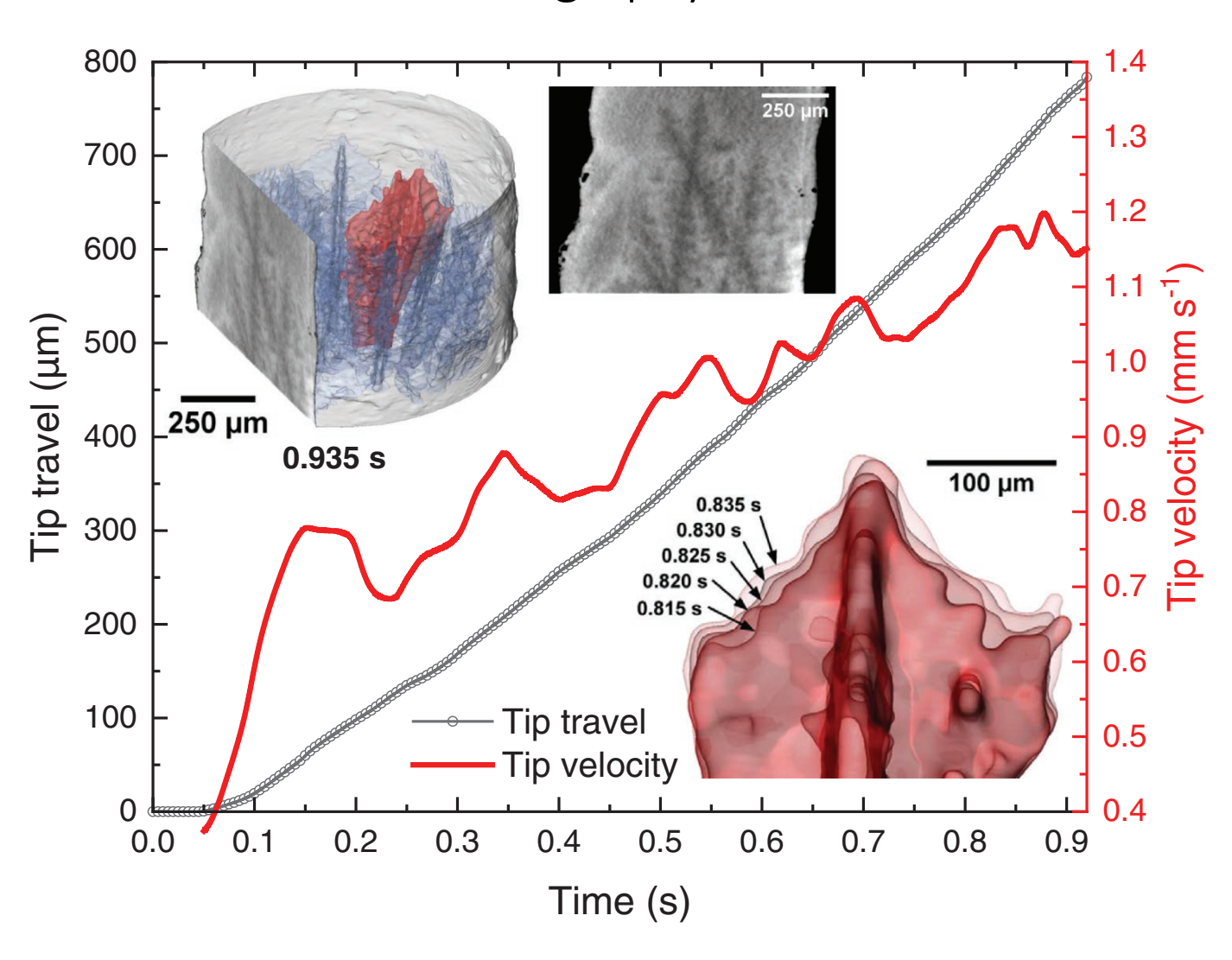


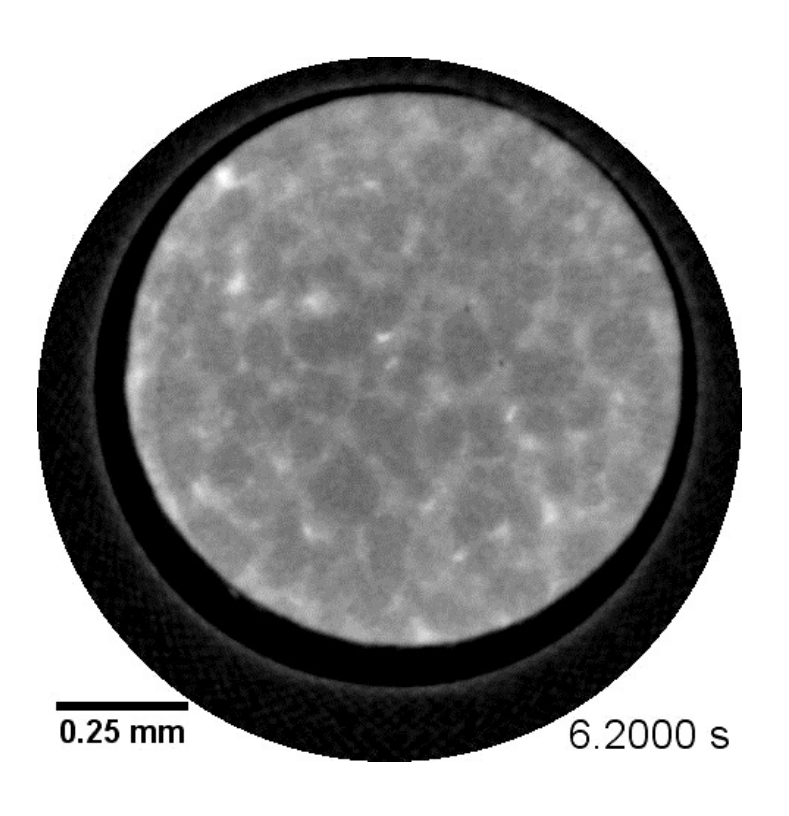


Solidification of AlBi10 (50 tps)

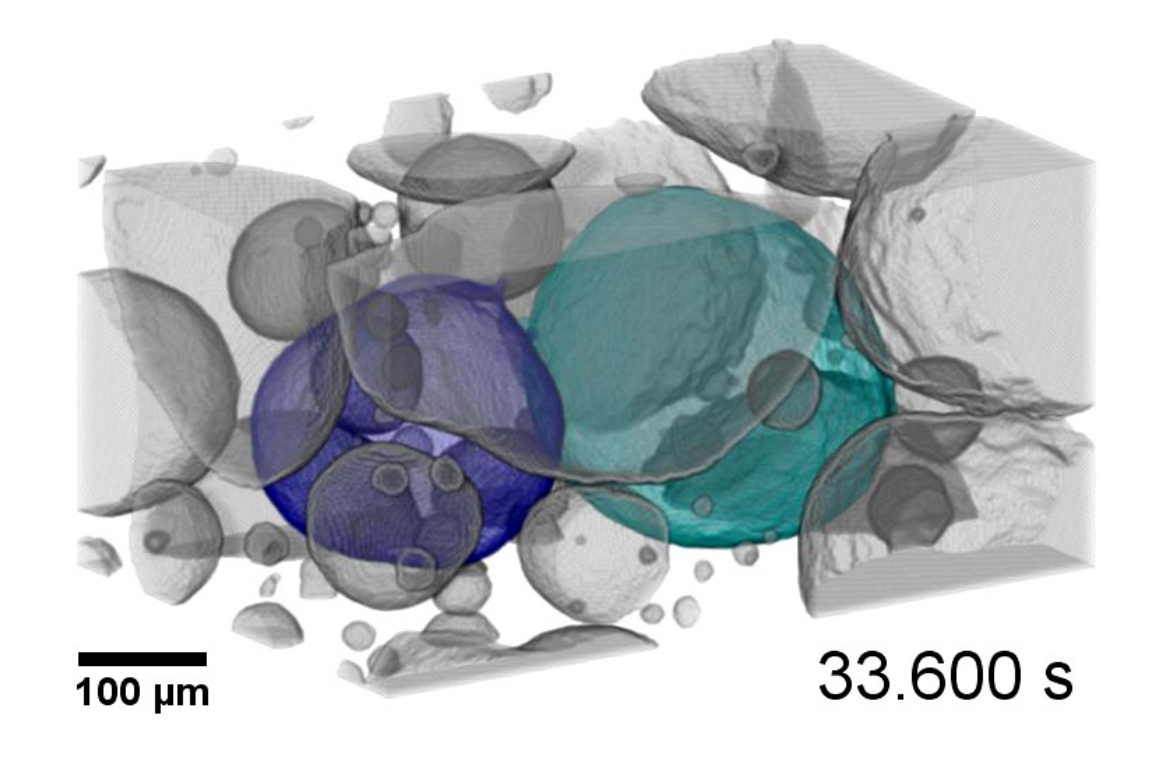
Solidification of AlGe10 (200 tps)

Burning of a sparkler (400 tps)







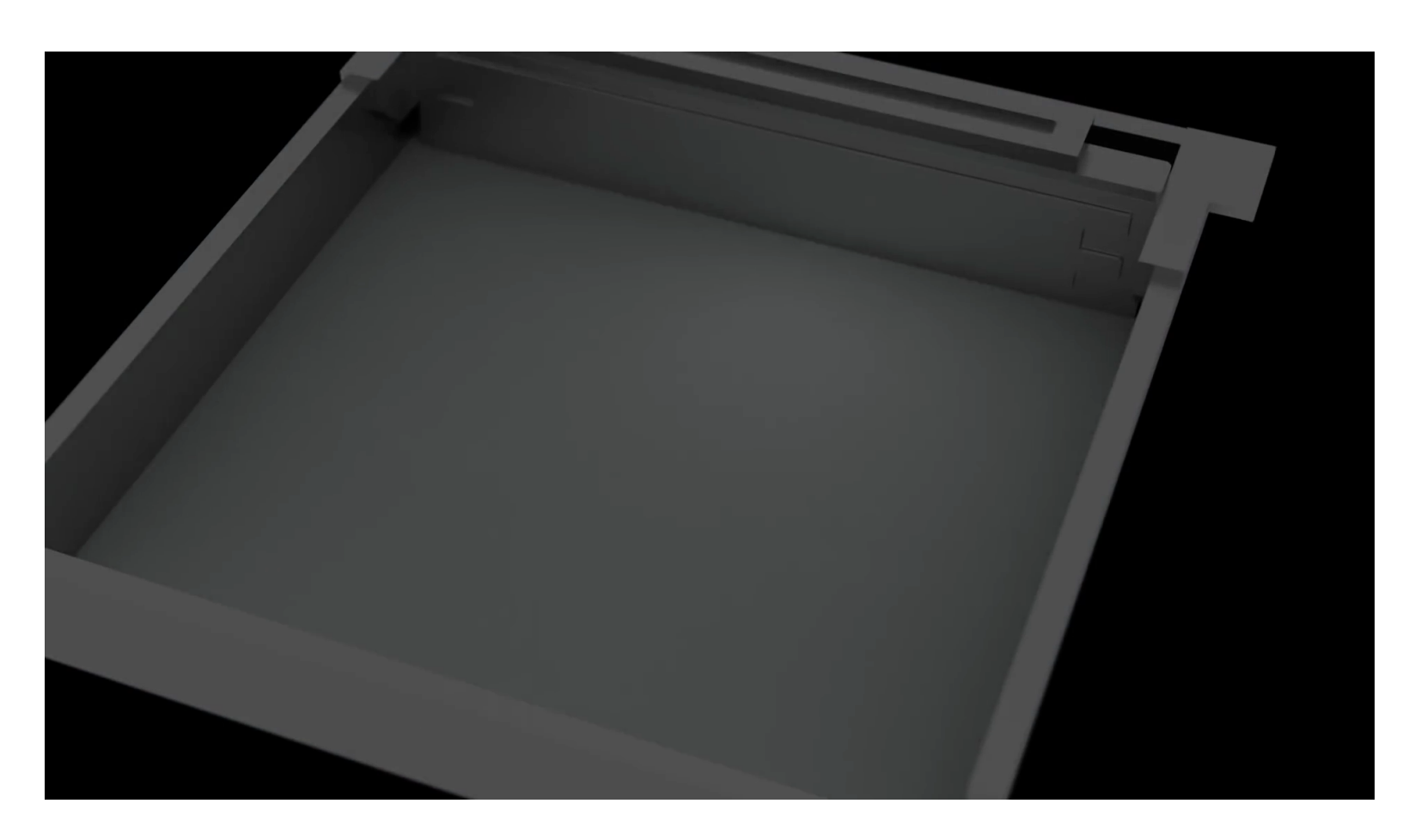


Coalescence of Bubbles in AlSi8Mg4 Alloy (1000 tps)

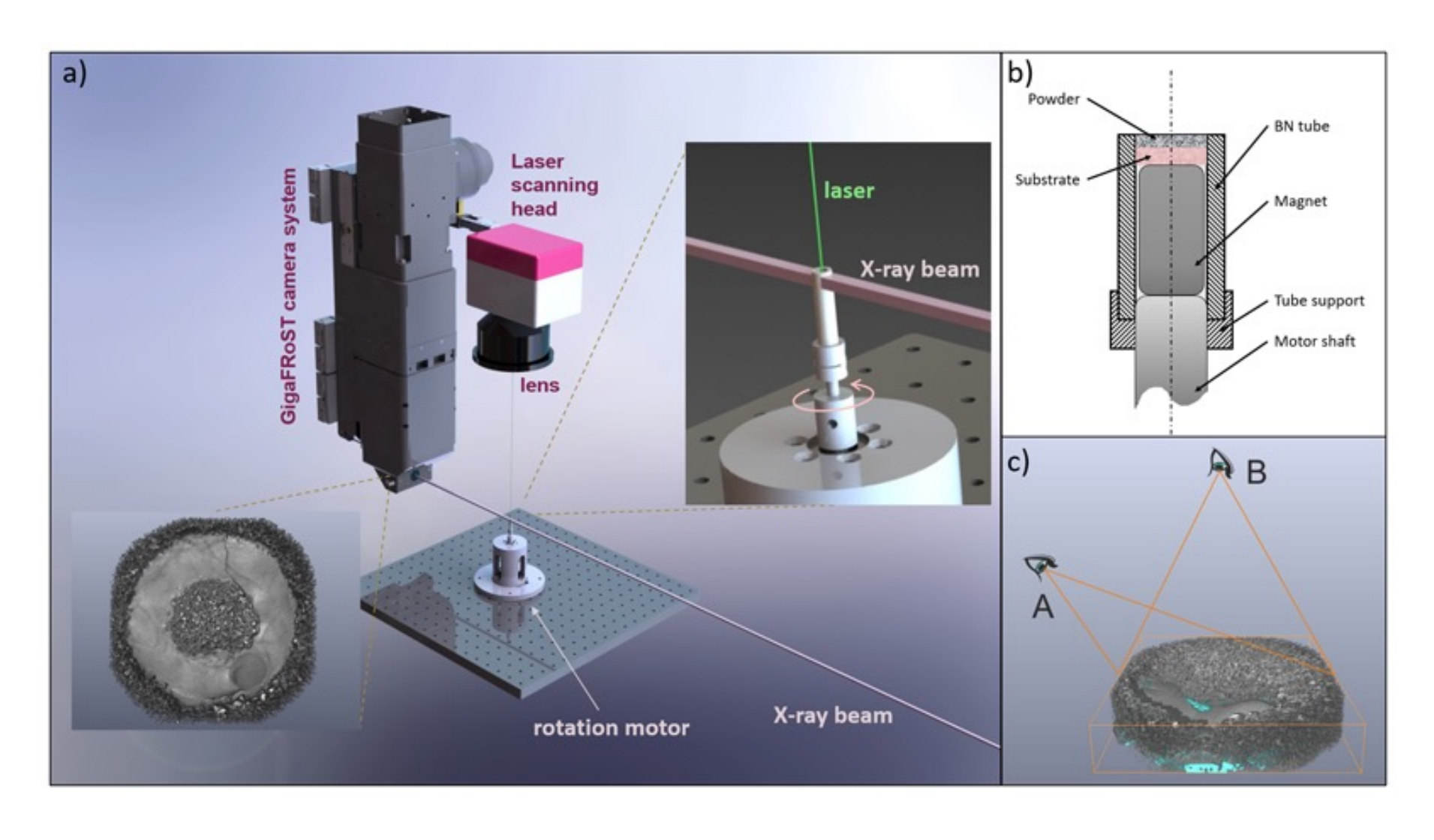
. .

Experiment ^{a)}	Tps $[s^{-1}]$	No. projections	Exposure [ms]	kfps	FoV [pixel]	No. of tomos	Raw file size [GB]	Rec. file size [GB]	Acceleration [g]
AlBi10	50	200	0.09	10	1008 × 400	3600	541	2725	2.5
AlGe10	200	100	0.045	20	528×280	11 801	331	1716	20.1
Sparkler	400	100	0.02	40	528 × 128	9501	121	1381	129
AlSi6Cu4 foam	650	62	0.02	40	480 × 128	44 354	315	2436	212
AlSi8Mg4 foam	1000	40	0.02	40	528 × 120	43 899	208	2735	503

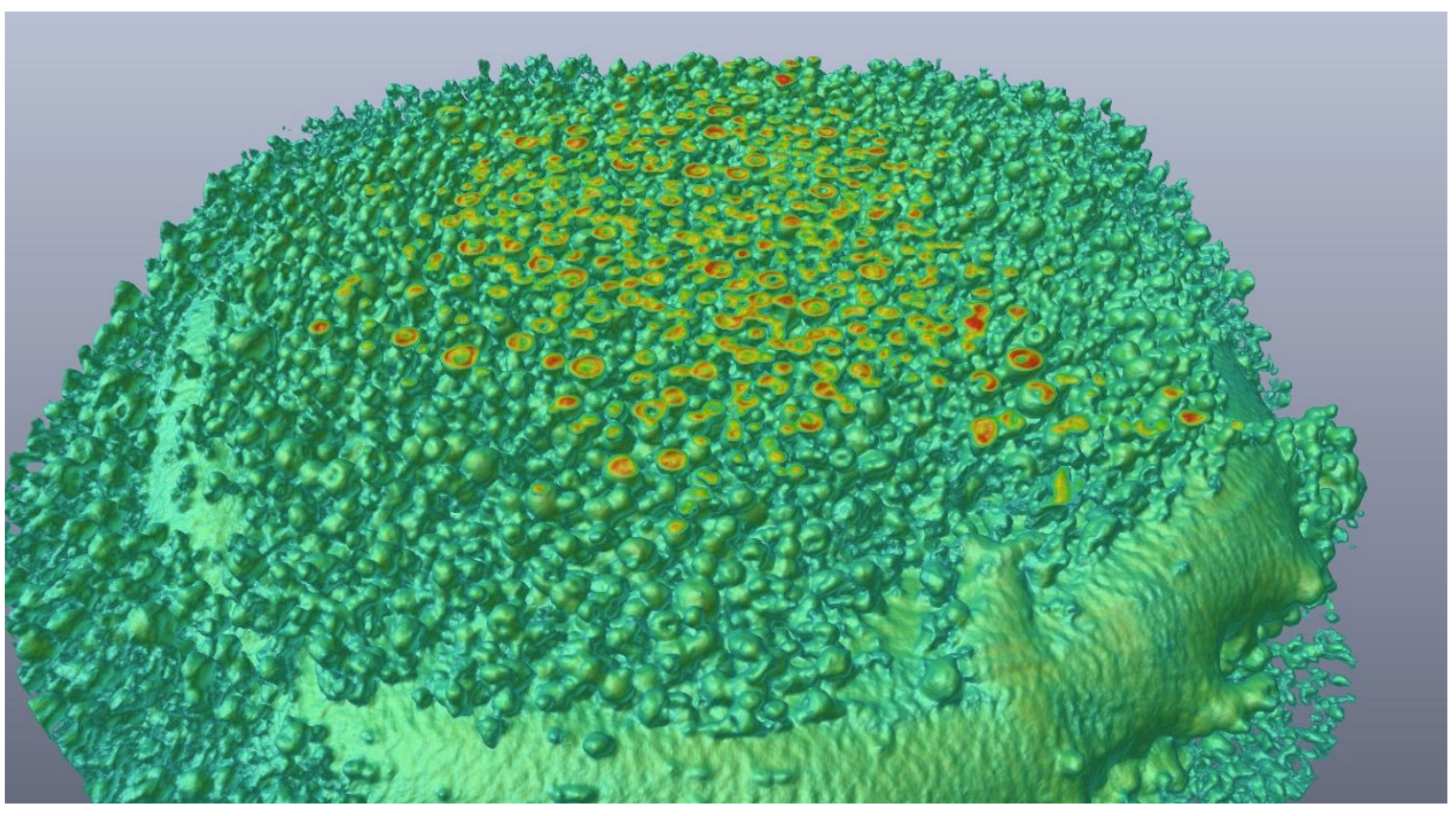
- Large g-forces can cause significant distortion
- Workarounds:
 - a multibeam approach with stationary samples
 - applying a reduced number of projections or limited angle acquisition, and combining with interlaced or intelligent reconstruction algorithms



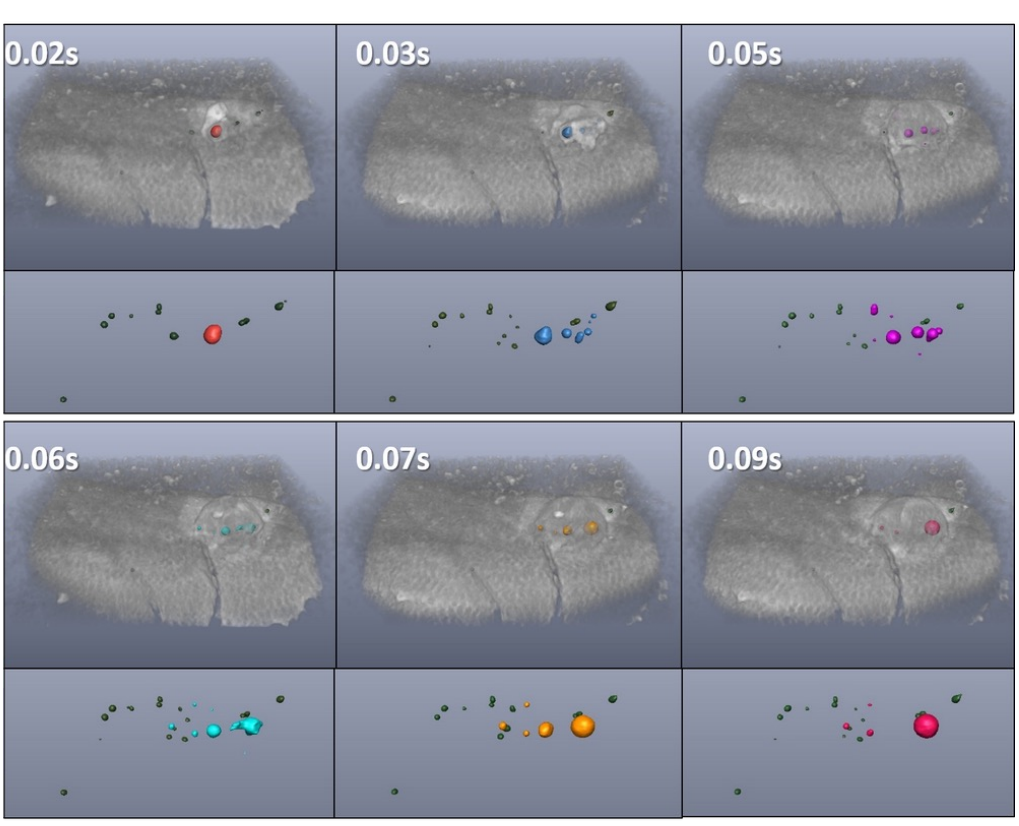
[SLM Solution GmbH - https://youtu.be/Mjf6oaMVWr8]





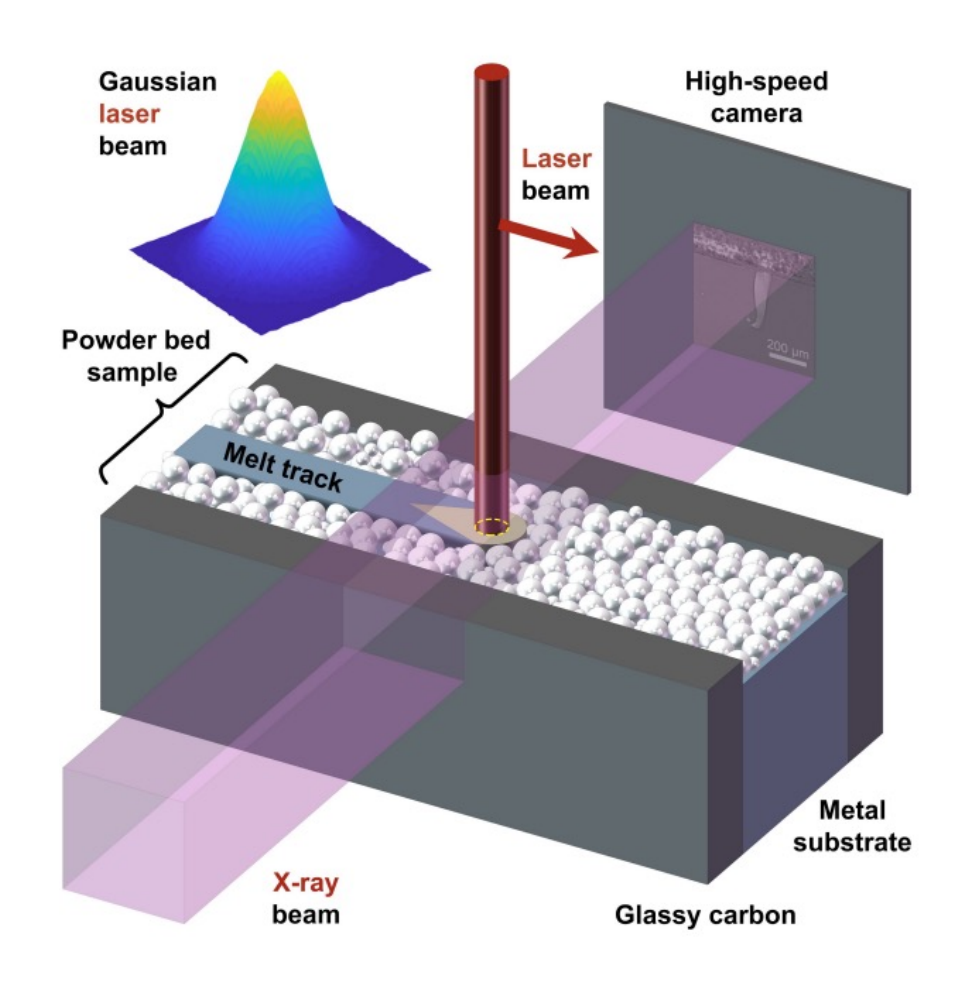


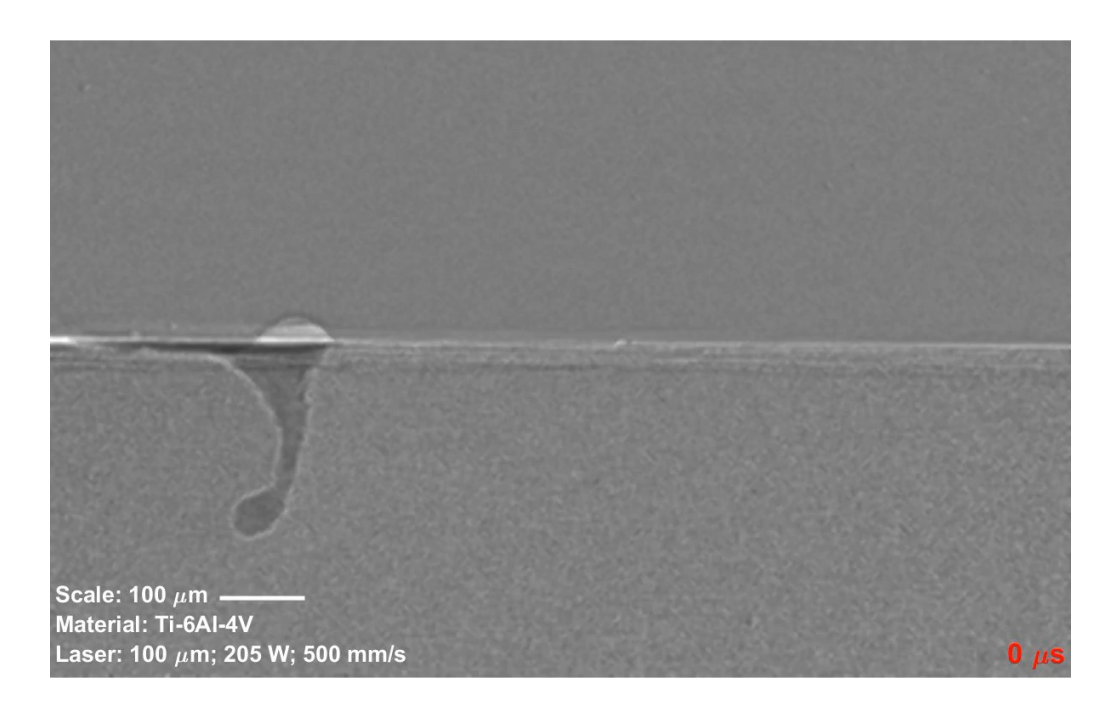




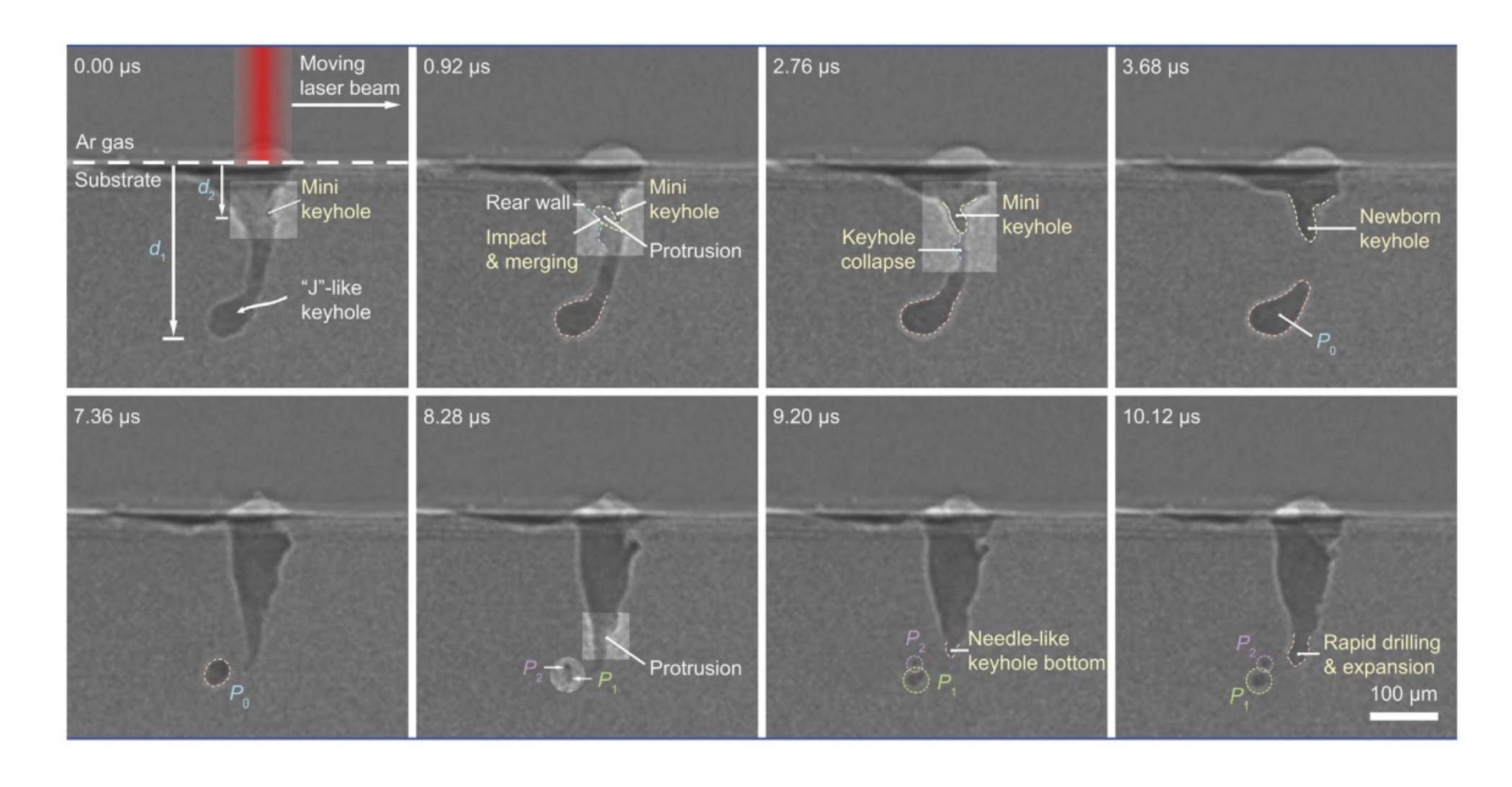
M. Makowska et al

Faster? In situ radiography during 3D printing



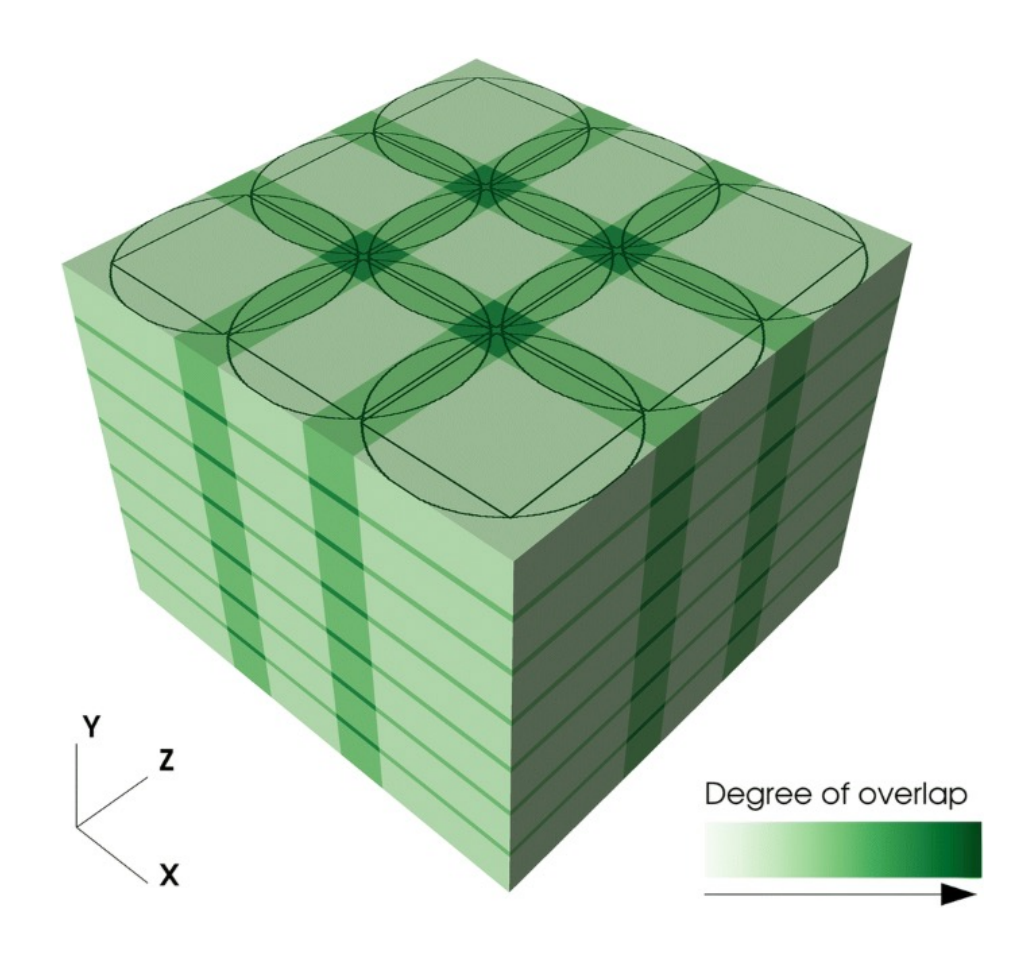


Faster? In situ radiography during 3D printing

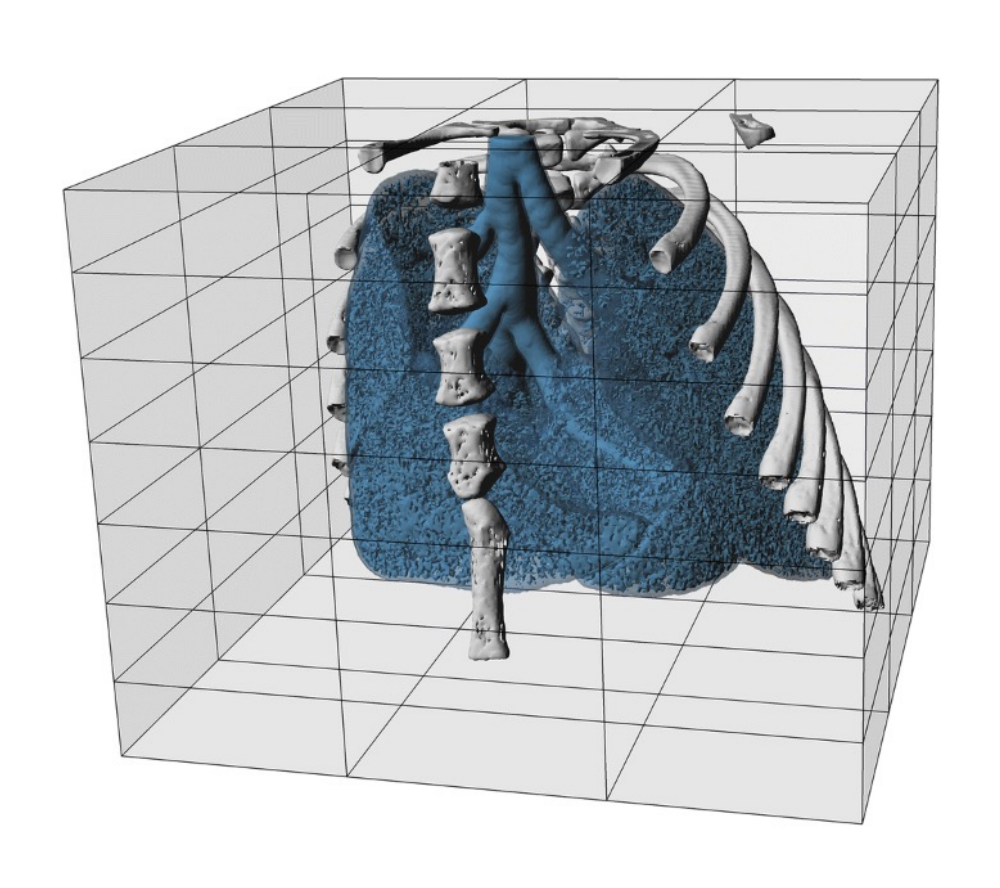


Larger? Field of view versus resolution

- Example: tomography of a rat lung
- Challenge: image within 20min with high resolution
- 3 x 3 x 7 tiles
- Final stitched 3D dataset consists of $9095 \times 9106 \times 7084$ voxels which corresponds to a physical volume of $25.0 \times 25.0 \times 19.5$ mm³
- The data size of the final stitched volume is about 1.2 TB



Field of view versus resolution

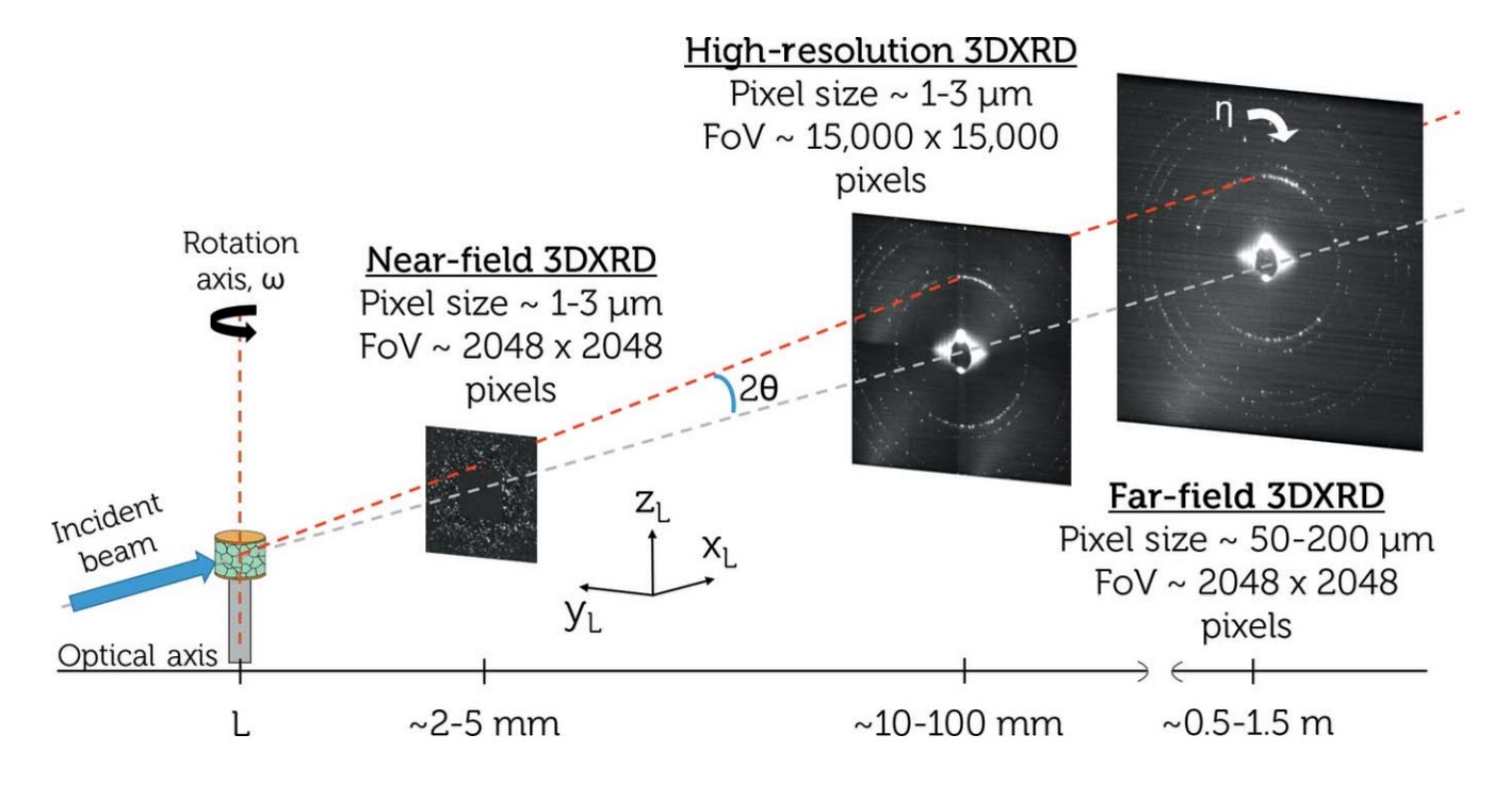




E. Borisova et al, Histochemistry and Cell Biology **155** (2021) 215–226

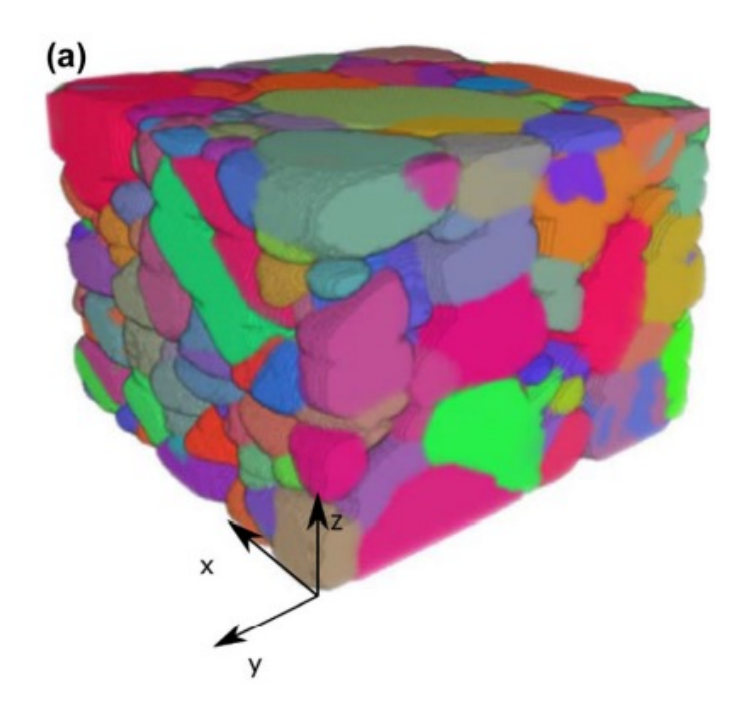
3DXRD

• 3DXRD is a far field diffraction technique capable of reconstructing polycrystalline materials from the individual diffraction spots recorded in the diffraction pattern given that the crystallographic parameters of the material are known



3DXRD

- In the near-field limit, the position of the `spot' on the detector is dominated by the real-space position and shape of the grain.
- In HR-3DXRD the detector is placed midfield, with $N_{\rm F}\simeq 1$, where a good compromise between linear and angular accuracy is obtained
- In far-field information on strain/stress is obtained



Space filling reconstruction of the grains